CHARACTERIZATION OF THE PTW MICROSILICON DETECTOR

By

Austin Turnidge

A THESIS

Presented to the Oregon Health & Science University
School of Medicine
in partial fulfillment of
the requirements for the degree of

Master of Science

June 2020

School of Medicine

Oregon Health & Science University

CERTIFICATE OF APPROVAL

This is to certify that the Master's thesis of

Austin Turnidge

has been approved

_____
Mentor/Advisor

_____
Member

_____
Member

_____
Member

TABLE OF CONTENTS

ACKNOWLEDGMENTS

Thank you to all parties who helped with this project: Malcolm Heard, Andrei Pugachev, Tyler Roberts, Richard Crilly, and Stephanie Junell.

ABSTRACT

According to Technical Report Series No. 483 (TRS 483), a detector that is used for large field dosimetry applications is assumed to be unacceptable for small field dosimetry applications until that detector has been adequately characterized specifically for small field dosimetry applications[1]. To do this for a silicon diode detector, its dose linearity, dose-per-pulse (DPP) dependence, effective point of measurement (EPOM), small field profiles, and small field output factors need to be measured for a variety of conditions that emulate the conditions in which the detector will actually be used. The PTW microSilicon is a silicon diode detector that has not been adequately characterized in the published literature for small field dosimetry applications.

Dose linearity, EPOM, small field profiles, and small field output factors were measured for all energies available on our TrueBeam. The microSilicon was shown to be DPP independent in a previous study[2]. Dose linearity was measured over a range of clinically relevant MU's for all energy/dose rate combinations. EPOM was measured using overlaid percent depth dose (PDD) scans taken with the microSilicon and microDiamond. Small field profiles were measured with the microSilicon and compared to those taken with the microDiamond. Small field output factors were measured with the microSilicon and compared to those taken with the W2.

A linear line of best fit was applied to each dose linearity measurement set: r^2 values were equal to or very close to 1.0000 for each measurement set. No shift was required to align the microSilicon's PDD scans to the microDiamond's PDD scans. For each 4 x 4 cm^2, 1 x 1 cm^2, and 0.5 x 0.5 cm^2 profile, the microSilicon had a field width within 0.5 mm of the microDiamond's

field width and the microSilicon had a penumbra width within 0.5 mm of the microDiamond's penumbra width.

The following conclusions have been made: (1) the microSilicon responds linearly with dose for all energy/dose rate combinations, (2) the microSilicon's nominal and measured EPOM's align, (3) the microSilicon is appropriate for measuring small photon field profiles down to a 0.5 x 0.5 cm^2 field size, (4) the microSilicon's performance is comparable to the microDiamond's performance for small photon field profile measurements down to a 0.5 x 0.5 cm^2 field size, (5) the microSilicon's small field output factors are identical to the W2's small field output factors, (6) when the microSilicon's characteristics are considered, it is an appropriate option for small field dosimetry applications.

1. INTRODUCTION

Accurate small field dosimetry is required to commission accurate stereotactic radiotherapy (SRT) and intensity-modulated radiotherapy (IMRT) modalities. The perturbation of charged particle fluence due to the presence of a detector, volume averaging effects, and the lack of lateral charged particle equilibrium make accurate small field dosimetry challenging[1].

Silicon diode detectors are a typical option for small field dosimetry applications. The PTW microSilicon is a waterproof unshielded silicon diode detector: it can be used for in-tank measurements of small photon fields and all electron fields[3].

According to TRS 483, a detector that is used for large field dosimetry applications is assumed to be unacceptable for small field dosimetry applications until that detector has been adequately characterized specifically for small field dosimetry applications[1]. To do this for a silicon diode detector, its dose linearity, DPP dependence, EPOM, small field profiles, and small field output factors need to be measured for a variety of conditions that emulate the conditions in which the detector will actually be used.

Schönfeld et al. measured the microSilicon's dose linearity for 6MV photons using a Siemens Primus and concluded that the microSilicon's response was linear with dose over the tested dose range. The microSilicon's DPP dependence for 10MV photons was measured using Primus. It was concluded that the microSilicon is DPP independent over the tested DPP range. The microSilicon's EPOM for 6MV photons was measured using 10 x 10 cm^2 and 4 x 4 cm^2 field sizes. It was concluded that the microSilicon's EPOM is 0.7 ± 0.2 mm below the detector's tip. The microSilicon's small field profiles were measured using TrueBeam, 6MV photons, a 1.6 x 1.6 cm^2

field size, and a 0.6 x 0.6 cm^2 field size. It was concluded that those profiles agree with those taken with the microDiamond in penumbra regions. The microSilicon's small field correction factors were measured using a Siemens Artiste, 6MV photons, and field sizes from 0.5 x 0.5 cm^2 to 4 x 4 cm^2. Two authors of this study are employees of PTW[2]. Akino et al. built on the existing literature by measuring the microSilicon's small field output factors using 6MV, 6FFF, 10MV, and 10FFF photons, and by testing its temperature dependence and energy dependence. It was concluded that the microSilicon exhibits small temperature dependence and energy dependence[4].

For our clinic, an adequate characterization of the microSilicon for small field dosimetry applications includes measuring its dose linearity for all energy/dose rate combinations available on our TrueBeam. It also includes measuring the microSilicon's EPOM, small field profiles, and small field output factors for all energies available on our TrueBeam. The microSilicon was assumed to be DPP independent per the findings of Schönfeld et al. In this paper, our clinic's definition of an adequate characterization of the microSilicon for small field dosimetry applications has been performed.

2. BACKGROUND

2.1 Silicon diode detectors

Silicon diode detectors are commonly used for relative dosimetry. They are small, rugged, and respond instantaneously. Ion chambers respond slower than silicon diode detectors because the energy required to produce an electron-hole pair in silicon is 3.5 eV whereas the energy required to produce an ion pair in air is 34 eV. Additionally, silicon's density is 1800 times that of air, so the current produced per unit volume in silicon is much larger than the current produced per unit volume in air: a small amount of silicon can provide an adequate signal. The limitations of silicon diode detectors include energy dependence in photon beams, angular dependence, temperature dependence, and susceptibility to radiation damage. Silicon diode detectors are commonly made by doping a silicon crystal (four valence electrons) with boron (three valence electrons) to make a p-type region and with phosphorus (five valence electrons) to make an n-type region. A depletion region of neutral charge is created at the interface between the p-type and n-type regions. An electric field is created across that depletion region since it is sandwiched between p-type and n-type regions. When a silicon diode detector is irradiated, electrons are freed in the depletion region and set into motion by the electric field: a radiation-induced current is created in the depletion region. Depletion region is synonymous with sensitive volume for silicon diode detectors[5]. A simple schematic of a silicon diode detector is shown in Figure 1.

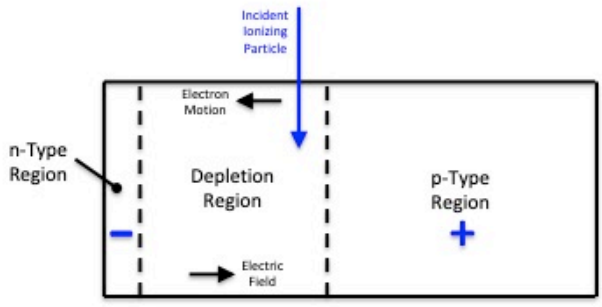

FIG. 1. Simple schematic of a silicon diode detector.

2.2 PTW microSilicon

The PTW microSilicon is an unshielded p-type silicon diode detector, which means that low energy scattered radiation contributes to recorded signals, that it can be used for electrons, and that it has a high level of p-type doping and a low level of n-type doping. A cross-section of the PTW microSilicon is shown in Figure 2.

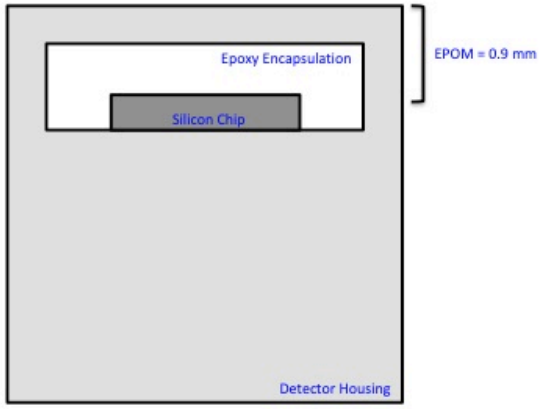

FIG. 2. Cross-section of the PTW microSilicon.

The microSilicon's sensitive volume has a radius of 0.75 mm and a thickness of 18 μm, its EPOM for photons is 0.9 mm from its tip, and it is designed to be used for for small photon field sizes and all electron field sizes[3].

2.3 PTW microDiamond

The PTW microDiamond is a synthetic diamond detector and it has advantages over silicon diode detectors, including very low temperature dependence, very low energy dependence, and very low dose rate dependence. Like the microSilicon, the microDiamond is also waterproof and can be used for photon and electron measurements. The microDiamond's sensitive volume has a radius

of 1.1 mm and a thickness of 1 μm, its EPOM for photons is 1 mm from its tip, and it is designed to be used for all photon field sizes and all electron field sizes[6].

2.4 Exradin W2

The Exradin W2 is a scintillator detector that can be used for both point dosimetry and scanning. It has a dedicated Cerenkov-correcting electrometer system, and has advantages over silicon diode detectors, including negligible temperature dependence, negligible energy dependence, and negligible dose rate dependence. The Exradin W2 has a small field output correction factor (k_Q) of 1.000, which makes it ideal for calculating its small field output factors $(\Omega's)$ and those of other detectors using TRS 483 methodology[7].

3. MATERIALS AND METHODS

All measurements were performed using our TrueBeam and its commissioned energies: 6MV, 6FFF, 10MV, & 10FFF. All plots were generated via MATLAB. Multiple signals were recorded then averaged for all measurements that were not scans.

3.1 Dose linearity

For dose linearity measurements, the microSilicon was coupled to a PTW BEAMSCAN tank and a Standard Imaging SuperMAX electrometer. The microSilicon was positioned in parallel orientation on central axis using the BEAMSCAN's auto setup procedure. For 6MV and 6FFF dose linearity measurements, the setup shown in Figure 3 left was used. For 10MV and 10FFF dose linearity measurements, the setup shown in Figure 3 right was used.

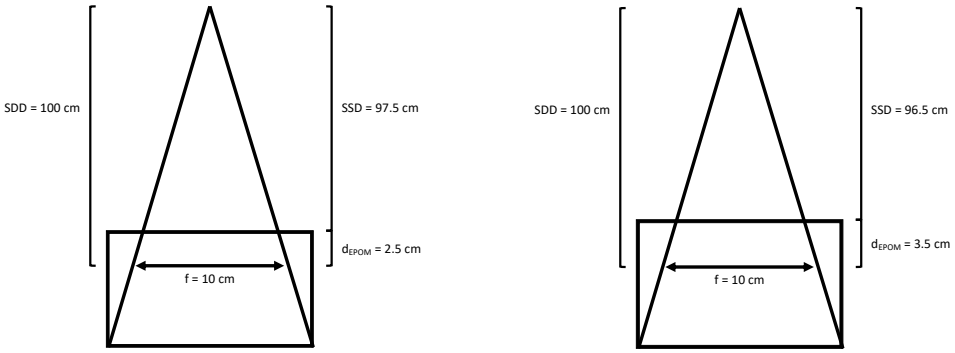

FIG. 3. Left: 6MV & 6FFF dose linearity measurement setup. Right: 10MV & 10FFF dose linearity measurement setup. Note: field sizes for all dose linearity measurements were jaw-defined.

Signals were recorded over a range of clinically relevant MU's for all energy/dose rate combinations available on our TrueBeam. Dose linearity plots were made using these recorded signals. Table 1 details each specific measurement set that was performed.

TABLE 1. Dose linearity measurements sets.

Measurement Set	Energy	Dose Rate	Range of MU's	Range of Doses (cGy)
1	6MV	600 MU/min	1 – 1000	1.02 – 1020
2	6MV	500 MU/min	1 – 1000	1.02 – 1020
3	6MV	400 MU/min	1 – 1000	1.02 – 1020
4	6MV	300 MU/min	1 – 1000	1.02 – 1020
5	6MV	200 MU/min	1 – 1000	1.02 – 1020
6	6MV	100 MU/min	1 – 1000	1.02 – 1020
7	6MV	80 MU/min	1 – 1000	1.02 – 1020
8	6MV	60 MU/min	1 – 1000	1.02 – 1020
9	6MV	40 MU/min	1 – 1000	1.02 – 1020
10	6MV	20 MU/min	1 – 100	1.02 – 102
11	6MV	15 MU/min	1 – 50	1.02 – 51
12	6MV	10 MU/min	1 – 50	1.02 – 51
13	6MV	5 MU/min	1 – 50	1.02 – 51
14	6FFF	1400 MU/min	1 – 1000	1.02 – 1020
15	6FFF	1200 MU/min	1 – 1000	1.02 – 1020
16	6FFF	1000 MU/min	1 – 1000	1.02 – 1020
17	6FFF	800 MU/min	1 – 1000	1.02 – 1020
18	6FFF	600 MU/min	1 – 1000	1.02 – 1020
19	6FFF	400 MU/min	1 – 1000	1.02 – 1020
20	10MV	600 MU/min	1 – 1000	1.05 – 1050
21	10MV	500 MU/min	1 – 1000	1.05 – 1050
22	10MV	400 MU/min	1 – 1000	1.05 – 1050
23	10MV	300 MU/min	1 – 1000	1.05 – 1050
24	10MV	200 MU/min	1 – 1000	1.05 – 1050
25	10MV	100 MU/min	1 – 500	1.05 – 525
26	10MV	80 MU/min	1 – 100	1.05 – 105
27	10MV	60 MU/min	1 – 100	1.05 – 105
28	10MV	40 MU/min	1 – 100	1.05 – 105
29	10MV	20 MU/min	1 – 50	1.05 – 52.5
30	10MV	15 MU/min	1 – 50	1.05 – 52.5
31	10MV	10 MU/min	1 – 50	1.05 – 52.5
32	10MV	5 MU/min	1 – 20	1.05 – 21
33	10FFF	2400 MU/min	1 – 1000	1.04 – 1040
34	10FFF	2000 MU/min	1 – 1000	1.04 – 1040
35	10FFF	1600 MU/min	1 – 1000	1.04 – 1040
36	10FFF	1200 MU/min	1 – 1000	1.04 – 1040
37	10FFF	800 MU/min	1 – 1000	1.04 – 1040
38	10FFF	400 MU/min	1 – 1000	1.04 – 1040

MU's that were delivered for each measurement set were converted to dose as follows:

$$D_d = \dot{D}_d * \mu = \left(\dot{D}_{d_0} * ISF * F * DD\right) * \mu$$

Where $\dot{D}_{d_0}$ is the normalization condition of 1.000 cGy/MU at the depth of maximum dose for a standard SSD setup, ISF is the inverse square factor that corrects $\dot{D}_{d_0}$ for setups with nonstandard SSD's, F is the Mayneord factor that corrects the depth dose measured at a specified depth using

a standard SSD setup (DD) for setups with nonstandard SSD's, and μ is the number of MU's that are delivered from the linac.

For all 6MV dose linearity measurement done in this project:

$$ISF = \left(\frac{100+d_0}{SSD+d_0}\right)^2 = \left(\frac{100+1.5}{97.5+1.5}\right)^2 = 1.051$$

$$F = \frac{DD_{\substack{Isocentric\\Setup}}}{DD} = \left(\frac{D_d}{D_{d_0}}\right)_{\substack{Isocentric\\Setup}} * \left(\frac{D_{d_0}}{D_d}\right) = \left(\frac{SSD+d_0}{SSD+d}\right)^2_{\substack{Isocentric\\Setup}} * \left(\frac{SSD+d}{SSD+d_0}\right)^2$$

$$\Rightarrow \; F = \left(\frac{97.5+1.5}{100}\right)^2 * \left(\frac{100+2.5}{100+1.5}\right)^2 = 0.9995$$

$$DD = 0.97 \;\; (from\ the\ 6MV\ microSilicon\ PDD\ scan\ that\ was\ measured)$$

$$\dot{D}_d = \dot{D}_{d_0} * ISF * F * DD = 1.000(1.051)(0.9995)(0.97) = 1.02\ cGy/MU$$

$$D_d = \dot{D}_d * \mu = 1.02 * \mu$$

For all 6FFF dose linearity measurements done in this project:

$$ISF = \left(\frac{100 + d_0}{SSD + d_0}\right)^2 = \left(\frac{100 + 1.4}{97.5 + 1.4}\right)^2 = 1.051$$

$$F = \frac{DD_{\substack{Isocentric\\Setup}}}{DD} = \left(\frac{D_d}{D_{d_0}}\right)_{\substack{Isocentric\\Setup}} * \left(\frac{D_{d_0}}{D_d}\right) = \left(\frac{SSD+d_0}{SSD+d}\right)^2_{\substack{Isocentric\\Setup}} * \left(\frac{SSD+d}{SSD+d_0}\right)^2$$

$$\Rightarrow \; F = \left(\frac{97.5+1.4}{100}\right)^2 * \left(\frac{100+2.5}{100+1.4}\right)^2 = 0.9995$$

$$DD = 0.97 \;\; (from\ the\ 6FFF\ microSilicon\ PDD\ scan\ that\ was\ measured)$$

$$\dot{D}_d = \dot{D}_{d_0} * ISF * F * DD = 1.000(1.051)(0.9995)(0.97) = 1.02\ cGy/MU$$

$$D_d = \dot{D}_d * \mu = 1.02 * \mu$$

For all 10MV dose linearity measurement done in this project:

$$ISF = \left(\frac{100 + d_0}{SSD + d_0}\right)^2 = \left(\frac{100 + 2.3}{96.5 + 2.3}\right)^2 = 1.072$$

$$F = \frac{DD_{\substack{Isocentric \\ Setup}}}{DD} = \left(\frac{D_d}{D_{d_0}}\right)_{\substack{Isocentric \\ Setup}} * \left(\frac{D_{d_0}}{D_d}\right) = \left(\frac{SSD+d_0}{SSD+d}\right)^2_{\substack{Isocentric \\ Setup}} * \left(\frac{SSD+d}{SSD+d_0}\right)^2$$

$$\Rightarrow \; F = \left(\frac{96.5+2.3}{100}\right)^2 * \left(\frac{100+3.5}{100+2.3}\right)^2 = 0.9992$$

$$DD = 0.98 \;\; (from\ the\ 10MV\ microSilicon\ PDD\ scan\ that\ was\ measured)$$

$$\dot{D}_d = \dot{D}_{d_0} * ISF * F * DD = 1.000(1.072)(0.9992)(0.98) = 1.05\ cGy/MU$$

$$D_d = \dot{D}_d * \mu = 1.05 * \mu$$

For all 10FFF dose linearity measurement done in this project:

$$ISF = \left(\frac{100 + d_0}{SSD + d_0}\right)^2 = \left(\frac{100 + 2.2}{96.5 + 2.2}\right)^2 = 1.072$$

$$F = \frac{DD_{\substack{Isocentric \\ Setup}}}{DD} = \left(\frac{D_d}{D_{d_0}}\right)_{\substack{Isocentric \\ Setup}} * \left(\frac{D_{d_0}}{D_d}\right) = \left(\frac{SSD+d_0}{SSD+d}\right)^2_{\substack{Isocentric \\ Setup}} * \left(\frac{SSD+d}{SSD+d_0}\right)^2$$

$$\Rightarrow \; F = \left(\frac{96.5+2.2}{100}\right)^2 * \left(\frac{100+3.5}{100+2.2}\right)^2 = 0.9991$$

$$DD = 0.97 \;\; (from\ the\ 10FFF\ microSilicon\ PDD\ scan\ that\ was\ measured)$$

$$\dot{D}_d = \dot{D}_{d_0} * ISF * F * DD = 1.000(1.072)(0.9991)(0.97) = 1.04\ cGy/MU$$

$$D_d = \dot{D}_d * \mu = 1.04 * \mu$$

3.2 Effective point of measurement

For EPOM measurements, the microSilicon was coupled to the BEAMSCAN tank and its built-in electrometer. The microSilicon was positioned in parallel orientation on central axis using the BEAMSCAN's auto setup procedure. A PTW SemiFlex 3D was also coupled to the BEAMSCAN system for use as a reference detector. The vertical zero point of the BEAMSCAN system was defined using the microSilicon's nominal EPOM: 0.9 mm from detector's tip for photons. SSD was set to 100 cm, energy was set to 6MV, and PDD scans were measured for 10 x 10 cm^2 and 4 x 4 cm^2 jaw-defined field sizes. These PDD scans were twice smoothed via the BEAMSCAN system's software. The Task Group 53 report on quality assurance recommends smoothing raw data to remove artifacts of the measurement technique[8]. The PDD scan parameter settings shown in Table 2 were used. This process was repeated in order to measure PDD scans for 6FFF, 10MV, and 10FFF energies.

All PDD scans were then repeated using the microDiamond in place of the microSilicon. The vertical zero point of the BEAMSCAN system was redefined using the microDiamond's nominal EPOM: 1 mm from the detector's tip. The measured microSilicon and microDiamond PDD scans were then overlaid to determine if the microSilicon's measured and nominal EPOM's align.

TABLE 2. PDD scan parameter settings.

Parameter	Setting
Scan Type	Stepwise
Measurement Time	1.0 s
Range	0 – 150 mm
Step	1.0 mm for 0 – 40 mm, 4.0 mm for 40 – 150 mm
Speed	1 mm/s for 0 – 40 mm, 10 mm/s for 40 – 150 mm
Scan Direction	Deep-to-shallow

The scan parameters shown in Table 2 were selected based purely on pragmatic experimentation of which BEAMSCAN system scan parameters output the least noisy data.

3.3 Small field profiles

For small field profile measurements, the microSilicon was coupled to the BEAMSCAN tank and it's built-in electrometer. The microSilicon was positioned in parallel orientation on central axis using the BEAMSCAN's auto setup procedure. The SemiFlex 3D was also coupled to the BEAMSCAN system for use as a reference detector. The vertical zero point of the BEAMSCAN system was defined using the microSilicon's nominal EPOM: 0.9 mm from detector's tip for photons. SSD was set to 95 cm, the microSilicon was set to 5 cm deep, energy was set to 6MV, and inplane and crossplane profile scans were measured for 4 x 4 cm^2, 1 x 1 cm^2, and 0.5 x 0.5 cm^2 field sizes. Field sizes were jaw-defined for 4 x 4 cm^2 and 1 x 1 cm^2 profile scans and multileaf collimator (MLC)-defined for 0.5 x 0.5 cm^2 profile scans. Jaws were set to 0.8 x 0.8 cm^2 for 0.5 x 0.5 cm^2 MLC-defined profile scans. All these small field profile scans were twice smoothed via the BEAMSCAN system's software. The Task Group 53 report on quality assurance recommends smoothing raw data to remove artifacts of the measurement technique[8]. The profile scan parameter settings shown in Table 3 were used. This process was repeated in order to measure small field profiles for 6FFF, 10MV, and 10FFF energies.

All small field profile scans were then repeated using the microDiamond in place of the microSilicon. The vertical zero point of the BEAMSCAN system was redefined using the microDiamond's nominal EPOM: 1 mm from the detector's tip. The measured microSilicon and microDiamond small field profiles were then overlaid to determine if the microSilicon is appropriate, and comparable to the microDiamond, for small field profile measurements. Film was

not used for small field profile measurements in this project, nor was it used by Schönfeld et al. or Akino et al. in their characterizations of the microSilicon.

TABLE 3. Small field profile scan parameter settings.

Parameter	Setting
Scan Type	Stepwise
Measurement Time	0.2 s for 4 x 4 cm^2 Field Sizes, 1.0 s otherwise
Range	50 mm Symmetric for 4 x 4 cm^2 Field Sizes, 40 mm Symmetric otherwise
Step	0.1 mm

The scan parameters shown in Table 3 were selected based purely on pragmatic experimentation of which BEAMSCAN system scan parameters output the least noisy data.

3.4 Small field output factors

For small field output factor measurements, the microSilicon was coupled to the BEAMSCAN tank and the SuperMAX electrometer. The microSilicon was positioned in parallel orientation on central axis using the BEAMSCAN's auto setup procedure. The vertical zero point of the BEAMSCAN system was defined using the microSilicon's nominal EPOM: 0.9 mm from the detector's tip for photons. SSD was set to 90 cm, the microSilicon was set to 10 cm deep, energy was set to 6MV, and signals were recorded for 10 x 10 cm^2, 4 x 4 cm^2, 2 x 2 cm^2, 1 x 1 cm^2, and 0.5 x 0.5 cm^2 field sizes. All field sizes were jaw-defined except 0.5 x 0.5 cm^2, which was MLC-defined with the jaws set to 0.8 x 0.8 cm^2. These measurements were repeated for 6FFF, 10MV, and 10FFF energies. This process was then repeated using the Exradin W2 (Standard Imaging, Middleton, WI, USA) in place of the microSilicon. W2 measurements were done in-tank using its dedicated Cerenkov-correcting electrometer system. The microSilicon and W2 measurements

were used to calculate small field output factors ($\Omega's$) for the microSilicon and W2 using TRS 483 methodology[1].

For example, the microSilicon's small field output factor for 6MV photons delivered with a 1 x 1 cm^2 field size $\left(\Omega_{Q_{clin},Q_{msr}}^{f_{clin},f_{msr}}\right)$ was calculated as:

$$\Omega_{Q_{clin},Q_{msr}}^{f_{clin},f_{msr}} = \frac{D_{w,Q_{clin}}^{f_{clin}}}{D_{w,Q_{msr}}^{f_{msr}}} = \frac{M_{Q_{clin}}^{f_{clin}}}{M_{Q_{msr}}^{f_{msr}}} k_{Q_{clin},Q_{msr}}^{f_{clin},f_{msr}}$$

Where $D_{w,Q_{clin}}^{f_{clin}}$ is the absorbed dose to water for the 6MV photons delivered with a 1 x 1 cm^2 field size, $D_{w,Q_{msr}}^{f_{msr}}$ is the absorbed dose to water for 6MV photons delivered with the reference field size (10 x 10 cm^2), $M_{Q_{clin}}^{f_{clin}}$ is the microSilicon's recorded signal for 6MV photons delivered with a 1 x 1 cm^2 field size, $M_{Q_{msr}}^{f_{msr}}$ is the microSilicon's recorded signal for 6MV photons delivered with the reference field size, and $k_{Q_{clin},Q_{msr}}^{f_{clin},f_{msr}}$ is the microSilicon's output correction factor for 6MV photons delivered with a 1 x 1 cm^2 field size.

To calculate the microSilicon's output correction factor for 6MV photons delivered with a 1 x 1 cm^2 field size $\left(k_{Q_{clin},Q_{msr}}^{f_{clin},f_{msr}}\right)$, the following relationship was used:

$$k_{Q_{clin},Q_{msr}}^{f_{clin},f_{msr}} = \left(\frac{M_{Q_{clin}}^{f_{clin}}}{M_{Q_{msr}}^{f_{msr}}} k\right)_{ref} * \left(\frac{M_{Q_{msr}}^{f_{msr}}}{M_{Q_{clin}}^{f_{clin}}}\right)_{sfd}$$

Where $\left(M_{Q_{clin}}^{f_{clin}}\right)_{ref}$ is the W2's recorded signal for 6MV photons delivered with a 1 x 1 cm^2 field size, $\left(M_{Q_{msr}}^{f_{msr}}\right)_{ref}$ is the W2's recorded signal for 6MV photons delivered with the reference field size, k_{ref} is the W2's output correction factor: 1.000, $\left(M_{Q_{msr}}^{f_{msr}}\right)_{sfd}$ is the microSilicon's recorded

signal for 6MV photons delivered with the reference field size, and $\left(M_{Q_{clin}}^{f_{clin}}\right)_{sfd}$ is the microSilicon's recorded signal for 6MV photons delivered with a 1 x 1 cm^2 field size.

4. RESULTS

4.1 Dose linearity

Dose linearity plots are shown in Figures 19-22. A linear line of best fit was applied to each dose linearity measurement set: r^2 values were equal or very close to 1.0000 for all plots. The only plots that did not have an r^2 value equal to 1.0000 were the 6MV 200 MU/min dose linearity plot and the 6MV 5 MU/min dose linearity plot, which had r^2 values of 0.9988 and 0.9996 respectively. An example dose linearity plot is shown in Figure 4.

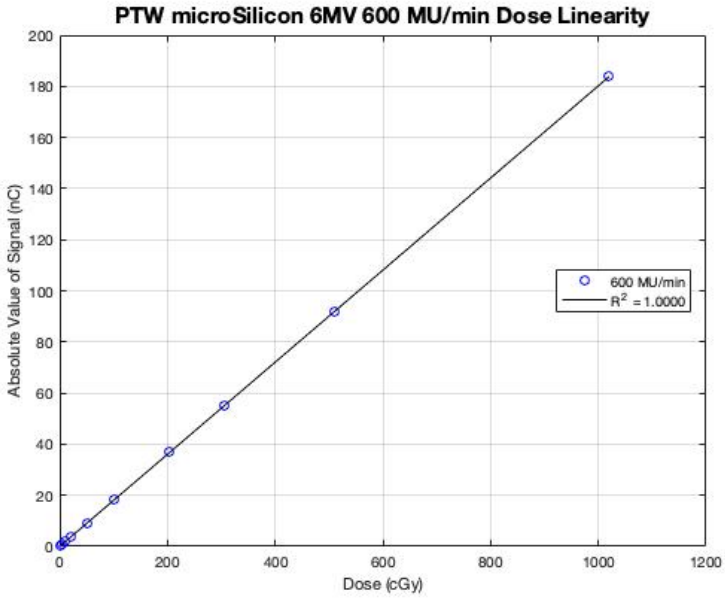

FIG. 4. Example dose linearity plot.

4.2 Effective point of measurement

6MV 10 x 10 cm^2 field size PDD scans measured with the microSilicon and microDiamond, and the relative difference of between the two detectors' normalized responses at each measurement point, are shown in Figure 5: the microSilicon's normalized response at 0 cm depth is 12.73% less than the microDiamond's normalized response at 0 cm depth, the microSilicon's normalized response at 1.5 cm depth (d_0) is equal to the microDiamond's normalized response at d_0, and the microSilicon's normalized response is within 1.00% of the microDiamond's normalized response past d_0. No shift was required to align the microSilicon's PDD scan to the microDiamond's PDD scan.

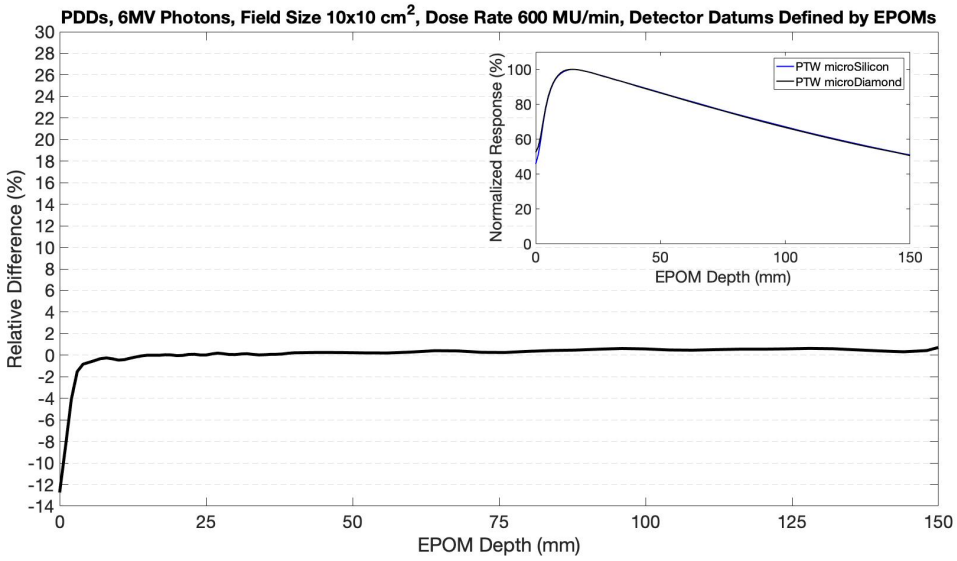

FIG. 5. 6MV 10 x 10 cm^2 field size EPOM measurement.

6MV 4 x 4 cm^2 field size PDD scans measured with the microSilicon and microDiamond, and the relative difference of between the two detectors' normalized responses at each measurement point, are shown in Figure 6: the microSilicon's normalized response at 0 cm depth is 9.26% less than the microDiamond's normalized response at 0 cm depth, the microSilicon's normalized response at 1.5 cm depth (d_0) is equal to the microDiamond's normalized response at d_0, and the microSilicon's normalized response is within 1.00% of the microDiamond's normalized response past d_0. No shift was required to align the microSilicon's PDD scan to the microDiamond's PDD scan.

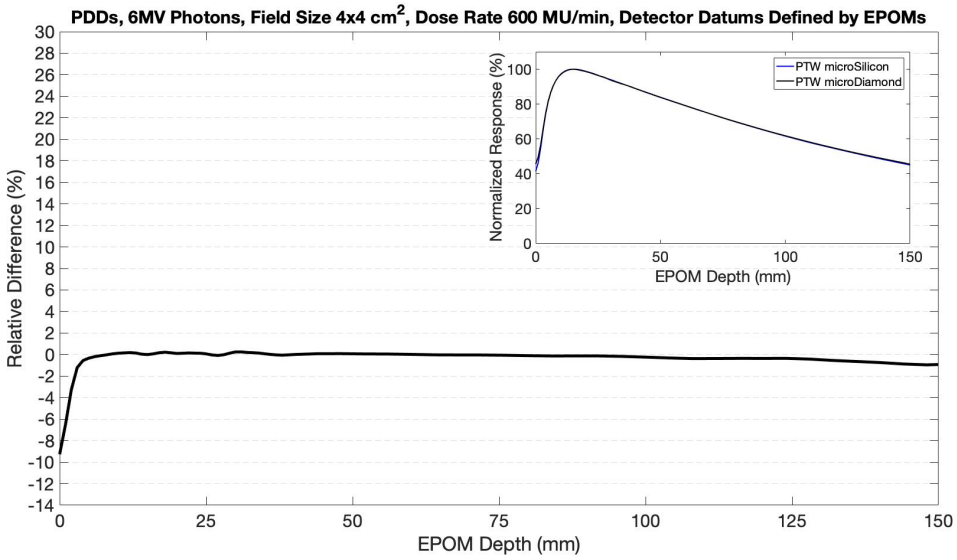

FIG. 6. 6MV 4 x 4 cm^2 field size EPOM measurement.

6FFF 10 x 10 cm^2 field size PDD scans measured with the microSilicon and microDiamond, and the relative difference of between the two detectors' normalized responses at each measurement point, are shown in Figure 7: the microSilicon's normalized response at 0 cm depth is 5.63% less than the microDiamond's normalized response at 0 cm depth, the microSilicon's normalized response at 1.4 cm depth (d_0) is equal to the microDiamond's normalized response at d_0, and the microSilicon's normalized response is within 1.00% of the microDiamond's normalized response past d_0. No shift was required to align the microSilicon's PDD scan to the microDiamond's PDD scan.

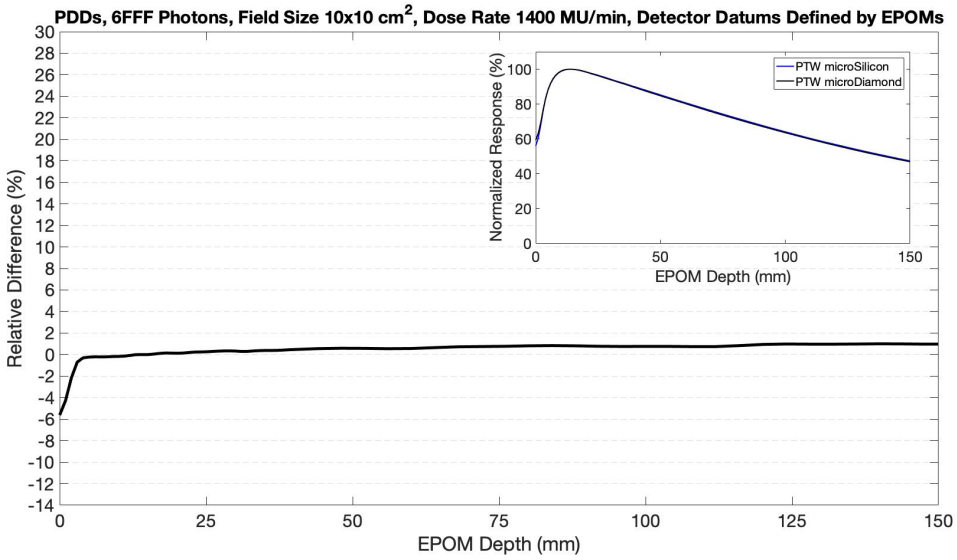

FIG. 7. 6FFF 10 x 10 cm^2 field size EPOM measurement.

6FFF 4 x 4 cm^2 field size PDD scans measured with the microSilicon and microDiamond, and the relative difference of between the two detectors' normalized responses at each measurement point, are shown in Figure 8: the microSilicon's normalized response at 0 cm depth is 6.55% less than the microDiamond's normalized response at 0 cm depth, the microSilicon's normalized response at 1.4 cm depth (d_0) is equal to the microDiamond's normalized response at d_0, and the microSilicon's normalized response is within 1.15% of the microDiamond's normalized response past d_0. No shift was required to align the microSilicon's PDD scan to the microDiamond's PDD scan.

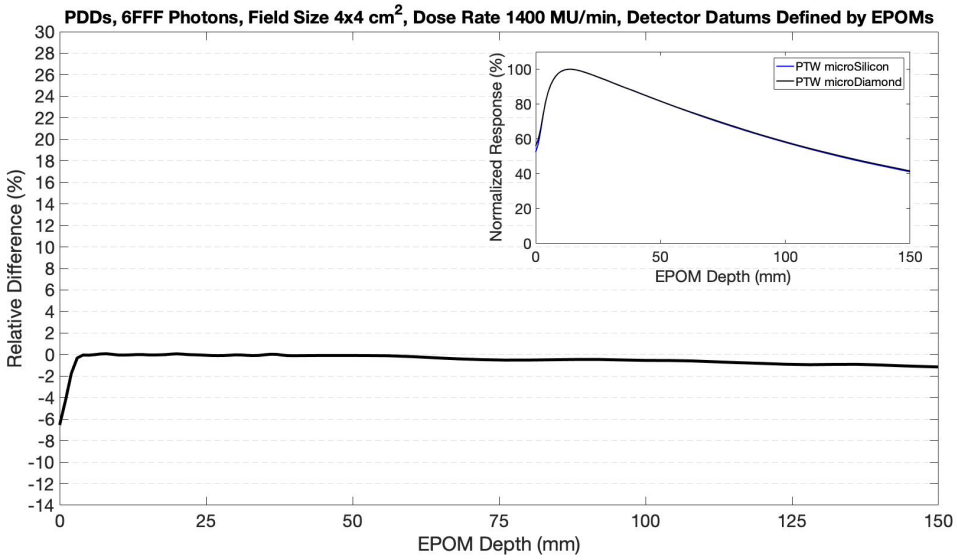

FIG. 8. 6FFF 4 x 4 cm^2 field size EPOM measurement.

10MV 10 x 10 cm^2 field size PDD scans measured with the microSilicon and microDiamond, and the relative difference of between the two detectors' normalized responses at each measurement point, are shown in Figure 9: the microSilicon's normalized response at 0 cm depth is 12.86% less than the microDiamond's normalized response at 0 cm depth, the microSilicon's normalized response at 2.3 cm depth (d_0) is 0.01% greater than the microDiamond's normalized response at d_0, and the microSilicon's normalized response is within 1.00% of the microDiamond's normalized response past d_0. No shift was required to align the microSilicon's PDD scan to the microDiamond's PDD scan.

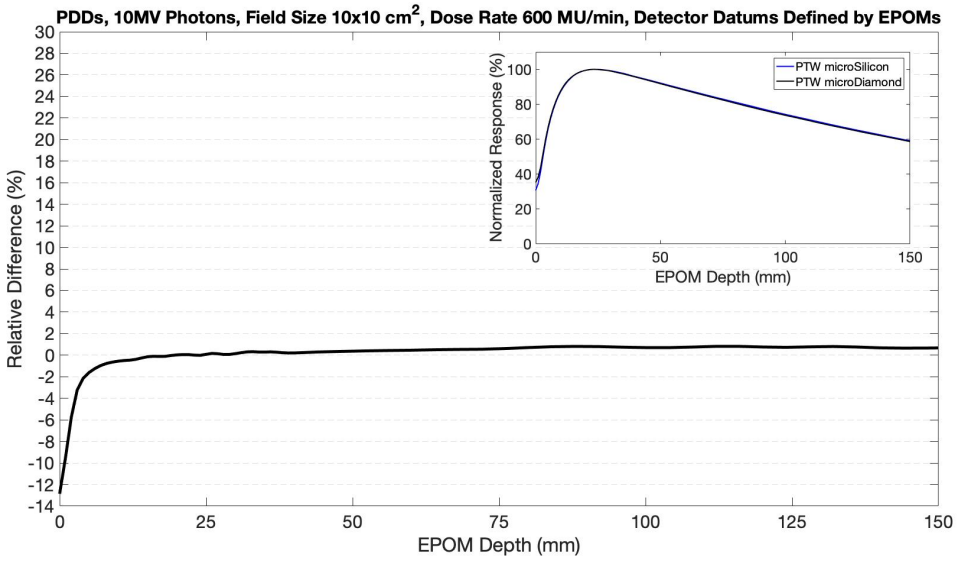

FIG. 9. 10MV 10 x 10 cm^2 field size EPOM measurement.

10MV 4 x 4 cm^2 field size PDD scans measured with the microSilicon and microDiamond, and the relative difference of between the two detectors' normalized responses at each measurement point, are shown in Figure 10: the microSilicon's normalized response at 0 cm depth is 16.21% less than the microDiamond's normalized response at 0 cm depth, the microSilicon's normalized response at 2.3 cm depth (d_0) is 0.01% less than the microDiamond's normalized response at d_0, and the microSilicon's normalized response is within 1.00% of the microDiamond's normalized response past d_0. No shift was required to align the microSilicon's PDD scan to the microDiamond's PDD scan.

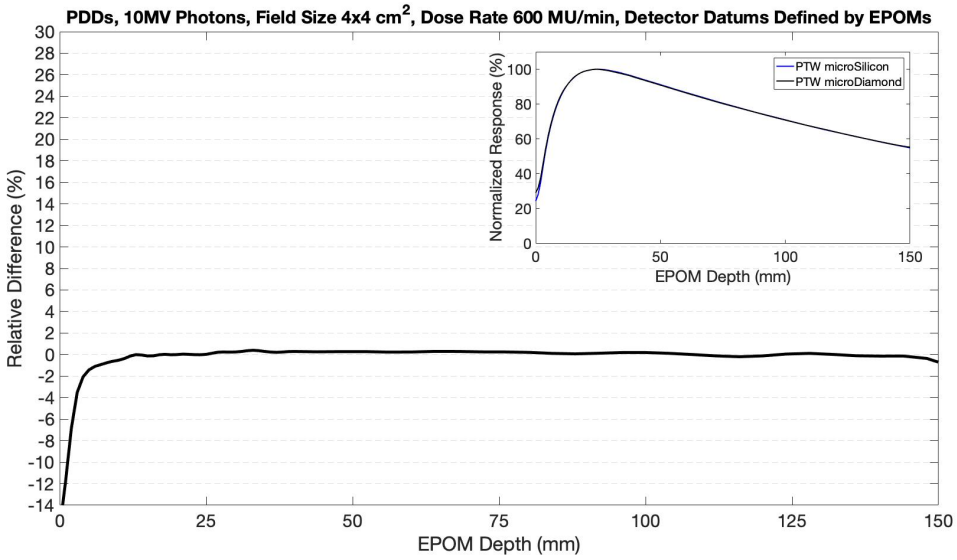

FIG. 10. 10MV 4 x 4 cm^2 field size EPOM measurement.

10FFF 10 x 10 cm^2 field size PDD scans measured with the microSilicon and microDiamond, and the relative difference of between the two detectors' normalized responses at each measurement point, are shown in Figure 11: the microSilicon's normalized response at 0 cm depth is 8.75% less than the microDiamond's normalized response at 0 cm depth, the microSilicon's normalized response at 2.2 cm depth (d_0) is equal to the microDiamond's normalized response at d_0, and the microSilicon's normalized response is within 1.00% of the microDiamond's normalized response past d_0. No shift was required to align the microSilicon's PDD scan to the microDiamond's PDD scan.

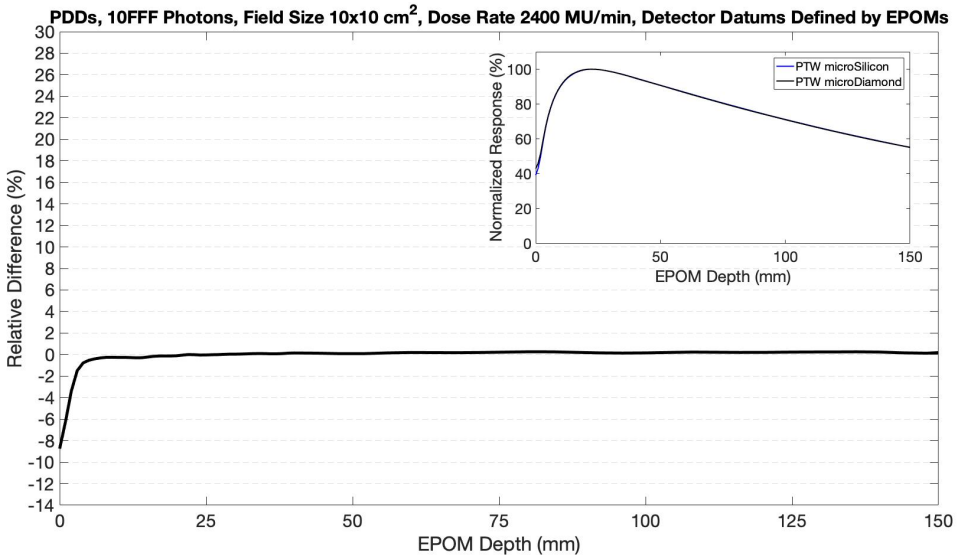

FIG. 11. 10FFF 10 x 10 cm^2 field size EPOM measurement.

10FFF 4 x 4 cm^2 field size PDD scans measured with the microSilicon and microDiamond, and the relative difference of between the two detectors' normalized responses at each measurement point, are shown in Figure 12: the microSilicon's normalized response at 0 cm depth is 8.63% less than the microDiamond's normalized response at 0 cm depth, the microSilicon's normalized response at 2.2 cm depth (d_0) is 0.04% greater than the microDiamond's normalized response at d_0, and the microSilicon's normalized response is within 1.00% of the microDiamond's normalized response past d_0. No shift was required to align the microSilicon's PDD scan to the microDiamond's PDD scan.

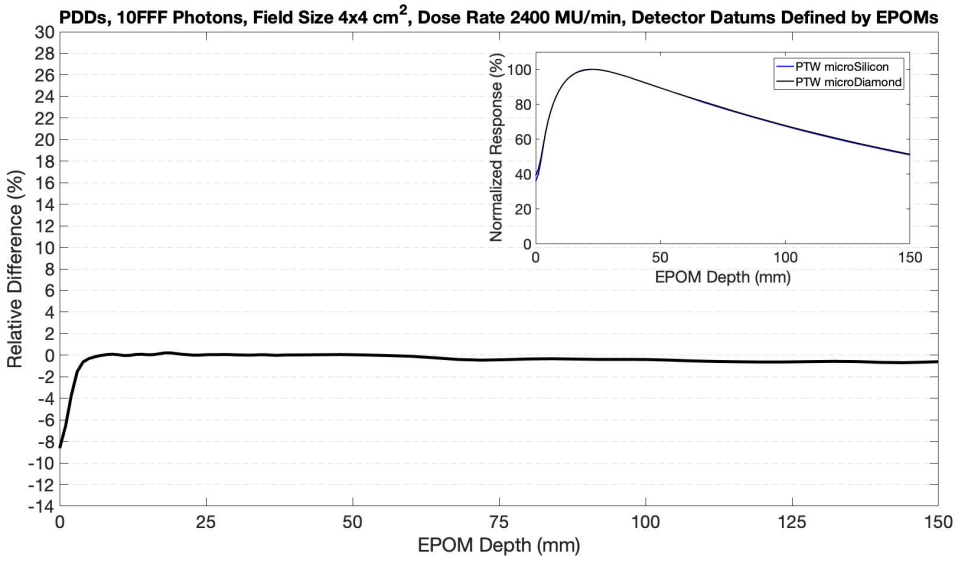

FIG. 12. 10FFF 4 x 4 cm^2 field size EPOM measurement.

4.3 Small field profiles

Small field profiles measured with the microSilicon and microDiamond are shown in Figures 23-46. All 4 x 4 cm^2, 1 x 1 cm^2, and 0.5 x 0.5 cm^2 field size profiles measured with the microSilicon had field widths within 0.5 mm of those measured with the microDiamond. Additionally, all 4 x 4 cm^2, 1 x 1 cm^2, and 0.5 x 0.5 cm^2 profiles measured with the microSilicon had penumbra widths within 0.5 mm of those measured with the microDiamond. An example small field profile measurement is shown in Figure 13.

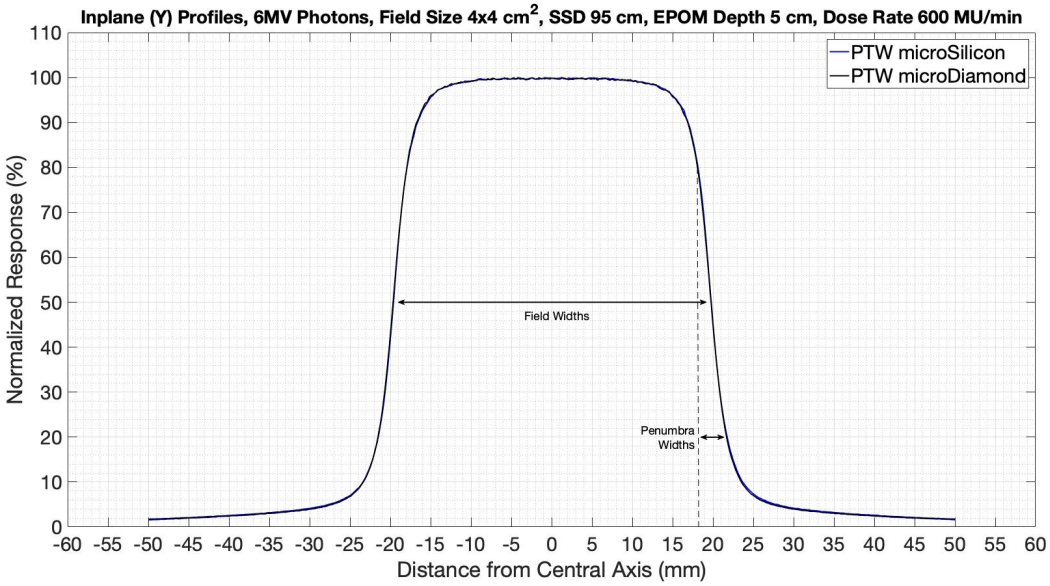

FIG. 13. Example small field profile measurement.

4.4 Small field output factors

Small field output factors for the microSilicon and W2 are shown in Tables 4-7 and Figures 14-17. Small field output correction factors for the microSilicon are shown in Tables 8-9 and Figure 18.

TABLE 4. PTW microSilicon small field output factors normalized to a 10 x 10 cm^2 field size.

Energy	Field Size	Small Field Output Factor
6MV	4 x 4 cm^2	0.877
6MV	2 x 2 cm^2	0.809
6MV	1 x 1 cm^2	0.684
6MV	0.5 x 0.5 cm^2	0.549
6FFF	4 x 4 cm^2	0.887
6FFF	2 x 2 cm^2	0.819
6FFF	1 x 1 cm^2	0.701
6FFF	0.5 x 0.5 cm^2	0.580
10MV	4 x 4 cm^2	0.901
10MV	2 x 2 cm^2	0.807
10MV	1 x 1 cm^2	0.626
10MV	0.5 x 0.5 cm^2	0.473
10FFF	4 x 4 cm^2	0.930
10FFF	2 x 2 cm^2	0.847
10FFF	1 x 1 cm^2	0.675
10FFF	0.5 x 0.5 cm^2	0.530

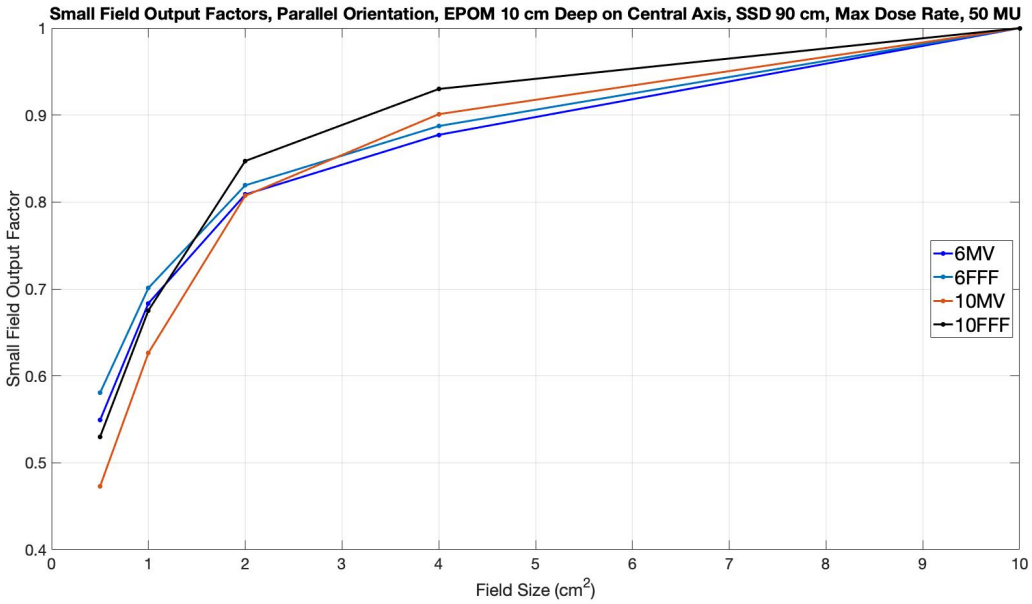

FIG. 14. PTW microSilicon small field output factors normalized to a 10 x 10 cm^2 field size.

TABLE 5. PTW microSilicon small field output factors normalized to a 4 x 4 cm^2 field size.

Energy	Field Size	Small Field Output Factor
6MV	4 x 4 cm^2	1.000
6MV	2 x 2 cm^2	0.922
6MV	1 x 1 cm^2	0.779
6MV	0.5 x 0.5 cm^2	0.626
6FFF	4 x 4 cm^2	1.000
6FFF	2 x 2 cm^2	0.923
6FFF	1 x 1 cm^2	0.790
6FFF	0.5 x 0.5 cm^2	0.654
10MV	4 x 4 cm^2	1.000
10MV	2 x 2 cm^2	0.896
10MV	1 x 1 cm^2	0.695
10MV	0.5 x 0.5 cm^2	0.525
10FFF	4 x 4 cm^2	1.000
10FFF	2 x 2 cm^2	0.911
10FFF	1 x 1 cm^2	0.726
10FFF	0.5 x 0.5 cm^2	0.570

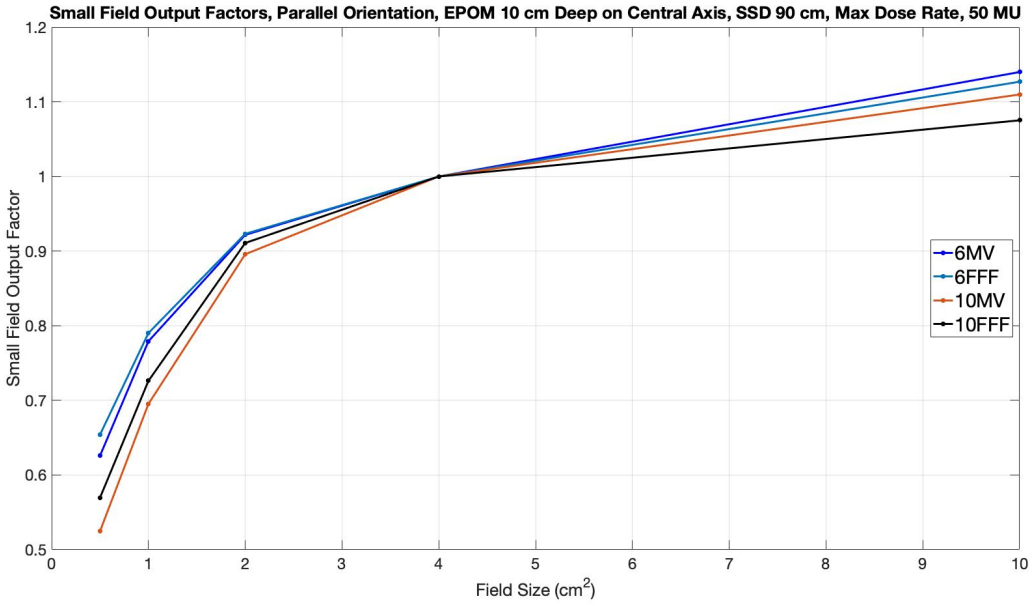

FIG. 15. PTW microSilicon small field output factors normalized to a 4 x 4 cm^2 field size.

TABLE 6. Exradin W2 small field output factors normalized to a 10 x 10 cm^2 field size.

Energy	Field Size	Small Field Output Factor
6MV	4 x 4 cm^2	0.877
6MV	2 x 2 cm^2	0.809
6MV	1 x 1 cm^2	0.684
6MV	0.5 x 0.5 cm^2	0.549
6FFF	4 x 4 cm^2	0.887
6FFF	2 x 2 cm^2	0.819
6FFF	1 x 1 cm^2	0.701
6FFF	0.5 x 0.5 cm^2	0.580
10MV	4 x 4 cm^2	0.901
10MV	2 x 2 cm^2	0.807
10MV	1 x 1 cm^2	0.626
10MV	0.5 x 0.5 cm^2	0.473
10FFF	4 x 4 cm^2	0.930
10FFF	2 x 2 cm^2	0.847
10FFF	1 x 1 cm^2	0.675
10FFF	0.5 x 0.5 cm^2	0.530

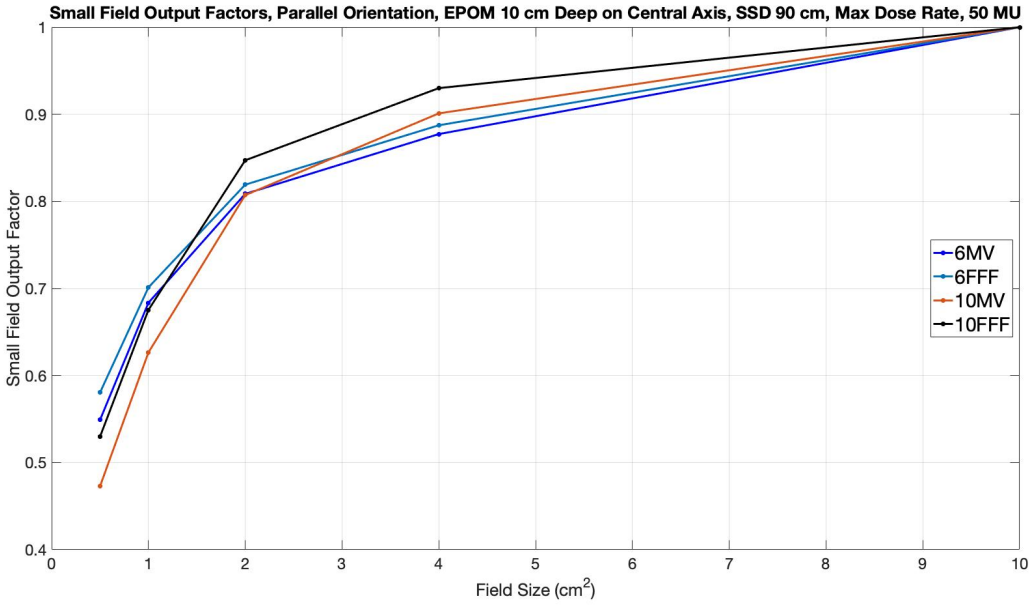

FIG. 16. Exradin W2 small field output factors normalized to a 10 x 10 cm^2 field size.

TABLE 7. Exradin W2 small field output factors normalized to a 4 x 4 cm^2 field size.

Energy	Field Size	Small Field Output Factor
6MV	4 x 4 cm^2	1.000
6MV	2 x 2 cm^2	0.922
6MV	1 x 1 cm^2	0.779
6MV	0.5 x 0.5 cm^2	0.626
6FFF	4 x 4 cm^2	1.000
6FFF	2 x 2 cm^2	0.923
6FFF	1 x 1 cm^2	0.790
6FFF	0.5 x 0.5 cm^2	0.654
10MV	4 x 4 cm^2	1.000
10MV	2 x 2 cm^2	0.896
10MV	1 x 1 cm^2	0.695
10MV	0.5 x 0.5 cm^2	0.525
10FFF	4 x 4 cm^2	1.000
10FFF	2 x 2 cm^2	0.911
10FFF	1 x 1 cm^2	0.726
10FFF	0.5 x 0.5 cm^2	0.570

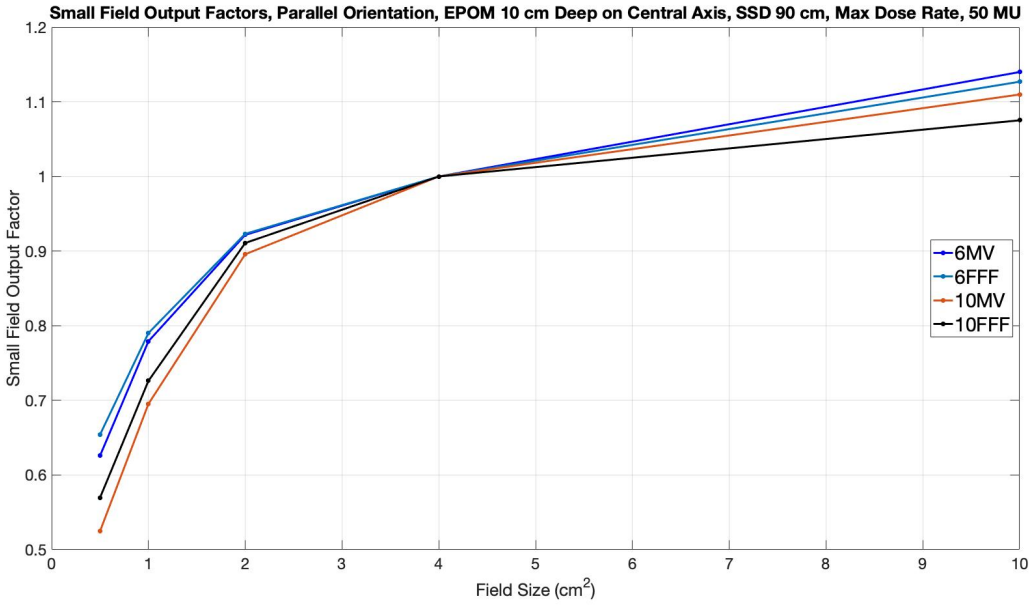

FIG. 17. Exradin W2 small field output factors normalized to a 4 x 4 cm^2 field size.

TABLE 8. PTW microSilicon small field output correction factors normalized to a 10 x 10 cm^2 field size.

Energy	Field Size	Small Field Output Correction Factor
6MV	4 x 4 cm^2	1.025
6MV	2 x 2 cm^2	1.033
6MV	1 x 1 cm^2	1.020
6MV	0.5 x 0.5 cm^2	1.014
6FFF	4 x 4 cm^2	1.027
6FFF	2 x 2 cm^2	1.036
6FFF	1 x 1 cm^2	1.025
6FFF	0.5 x 0.5 cm^2	1.018
10MV	4 x 4 cm^2	1.027
10MV	2 x 2 cm^2	1.030
10MV	1 x 1 cm^2	1.022
10MV	0.5 x 0.5 cm^2	1.025
10FFF	4 x 4 cm^2	1.023
10FFF	2 x 2 cm^2	1.028
10FFF	1 x 1 cm^2	1.019
10FFF	0.5 x 0.5 cm^2	1.017

TABLE 9. PTW microSilicon small field output correction factors normalized to a 4 x 4 cm^2 field size.

Energy	Field Size	Small Field Output Correction Factor
6MV	4 x 4 cm^2	1.000
6MV	2 x 2 cm^2	1.008
6MV	1 x 1 cm^2	0.995
6MV	0.5 x 0.5 cm^2	0.989
6FFF	4 x 4 cm^2	1.000
6FFF	2 x 2 cm^2	1.008
6FFF	1 x 1 cm^2	0.998
6FFF	0.5 x 0.5 cm^2	0.991
10MV	4 x 4 cm^2	1.000
10MV	2 x 2 cm^2	1.003
10MV	1 x 1 cm^2	0.995
10MV	0.5 x 0.5 cm^2	0.998
10FFF	4 x 4 cm^2	1.000
10FFF	2 x 2 cm^2	1.005
10FFF	1 x 1 cm^2	0.996
10FFF	0.5 x 0.5 cm^2	0.994

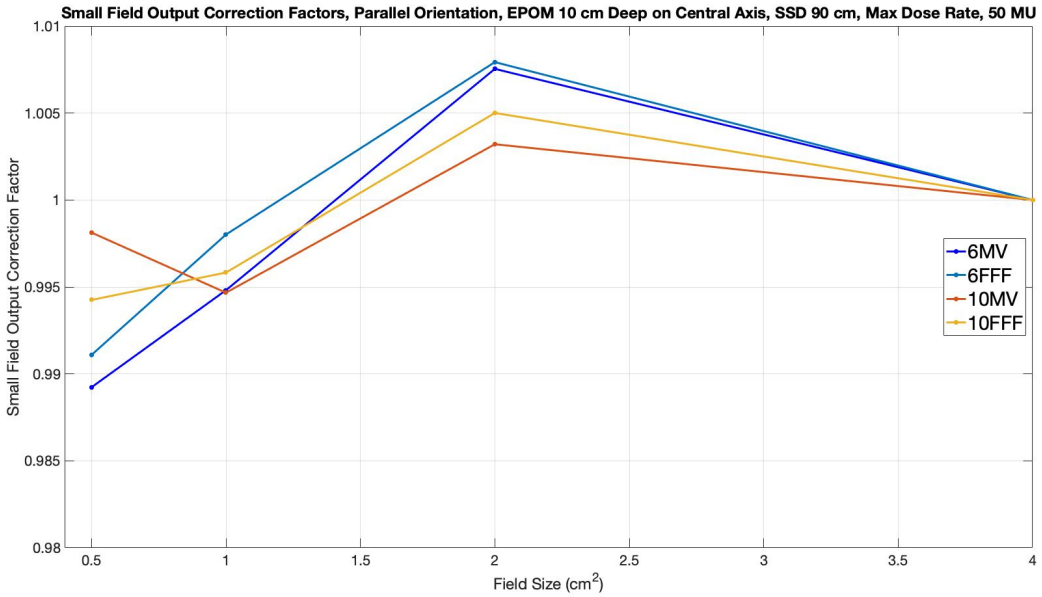

FIG. 18. PTW microSilicon small field output correction factors normalized to a 4 x 4 cm^2 field size.

5. DISCUSSION

5.1 Dose linearity

The 6MV 200 MU/min and 6MV 5 MU/min dose linearity data, which had r^2 values of 0.9988 and 0.9996 respectively, are still fitted extremely well with the applied linear lines of best fit.

5.2 Effective point of measurement

The microSilicon's normalized response at 0 cm depth is less than the microDiamond's normalized response at 0 cm depth for all measured PDD scans: more buildup was observed with the microDiamond than with the microSilicon. This makes sense because when the nominal EPOM of each detector is positioned at 0 cm depth, the microDiamond extends further above the water surface, causing more buildup. The microDiamond's measured PDD scans were assumed to be "true" PDD scans against which the microSilicon's measured PDD scans were compared, a shift between any set of PDD scans indicating a discrepancy between the microSilicon's nominal and measured EPOM's. Assuming that the microDiamond's measured PDD scans were "true" PDD scans is synonymous with assuming that the microDiamond's nominal and measured EPOM's align, both being 1 mm from the detector's tip. No shift was required to align any of the microSilicon's measured PDD scans to those measured with the microDiamond, indicating that the microSilicon's nominal and measured EPOM's align, both being 0.9 mm from the detector's tip.

5.3 Small field profiles

For each 4 x 4 cm^2, 1 x 1 cm^2, and 0.5 x 0.5 cm^2 profile, the microSilicon had a field width within 0.5 mm of the microDiamond's field width and the microSilicon had a penumbra width within 0.5 mm of the microDiamond's penumbra width. For these profile measurements, the microSilicon did not exhibit less volume averaging than the microDiamond (see Figures 23-46).

5.4 Small field output factors

The microSilicon's small field output factors are identical to the W2's small field output factors.

6. SUMMARY AND CONCLUSIONS

The microSilicon responds linearly with dose for all energy/dose rate combinations available on our TrueBeam. Its nominal and measured EPOM's align: both are 0.9 mm from the detector's tip. It's appropriate for measuring small photon field profiles down to a 0.5 x 0.5 cm^2 field size. The microSilicon's performance is comparable to the microDiamond's performance for small photon field profile measurements down to a 0.5 x 0.5 cm^2 field size. The microSilicon's small field output factors are identical to the W2's small field output factors. When the microSilicon's characteristics are considered, it is an appropriate option for small field dosimetry applications.

7. LIMITATIONS OF CONCLUSIONS

The conclusions detailed above are only valid for the specific test parameters that were used. For example, it was concluded that the microSilicon's performance is comparable to the microDiamond's performance for small field profile measurements down to a 0.5 x 0.5 cm^2 field size, which is only a valid conclusions for the tested dose rates (600 MU/min for 6MV small field profile measurements, 1400 MU/min for 6FFF small field profile measurements, 600 MU/min for 10MV small field profile measurements, and 2400 MU/min for 10FFF small field profile measurements) and not for higher does rates such as those used in FLASH radiotherapy.

8. FUTURE DIRECTIONS

The BEAMSCAN system scan parameters used for PDD scans and small field profile scans could be further refined in a future study. Specifically, those scan parameters could be optimized separately for the microSilicon and the microDiamond.

9. REFERENCES

1. IAEA Technical Report Series No. 483 (2017). Dosimetry of small static fields used in external beam radiotherapy. Vienna: IAEA.
2. Schönfeld, A.-B., Poppinga, D., Kranzer, R., De Wilde, R.L., Willborn, K., Poppe, B. and Looe, H.K. (2019). Technical Note: Characterization of the new microSilicon diode detector. Med. Phys., 46: 4257-4262.
3. microSilicon (n.d.). In *PTW*. Retrieved from https://www.ptwdosimetry.com/en/products/microsilicon/
4. Akino, Y., Fujiwara, M., Okamura, K., Shiomi, H., Mizuno, H., Isohashi, F., Suzuki, O., Seo, Y., Tamari, K., and Ogawa, K. (2020, May). Characterization of a microSilicon diode detector for small-field photon beam dosimetry. *Journal of Radiation Research*, *61*(3), 410-418.
5. Khan, F. M. (2010). *The Physics of Radiation Therapy* (Fourth ed.). Baltimore, MD: Lippincott Williams & Wilkins, a Wolters Kluwer business.
6. microDiamond (n.d.). In *PTW*. Retrieved from https://www.ptwdosimetry.com/en/products/microdiamond/
7. Scintillators (n.d.). In *Standard Imaging.* Retrieved from https://www.standardimaging.com/exradin/scintillators
8. Fraass, B., Doppke, K., Hunt, M., Kutcher, G., Starkschall, G., Stern, R., Van Dyke, J. (1998). American Association of Physicists in Medicine Radiation Therapy Committee Task Group 53: Quality assurance for clinical radiotherapy treatment planning. Med. Phys., 25: 1773-1829.

10. APPENDIX

10.1 Dose linearity

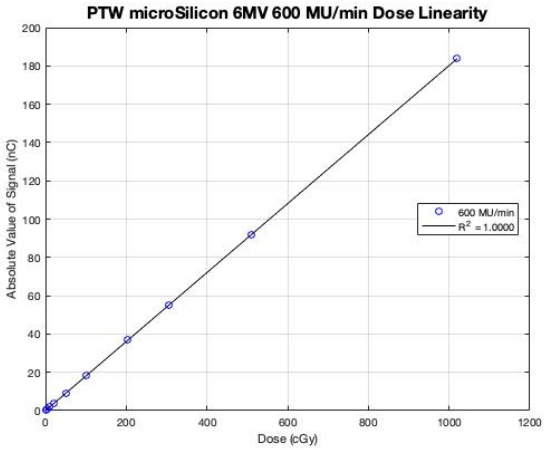

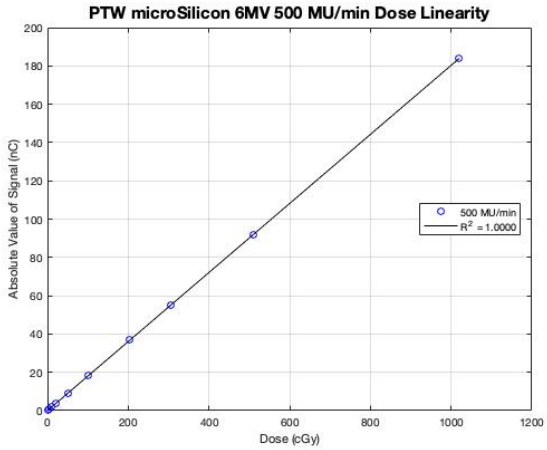

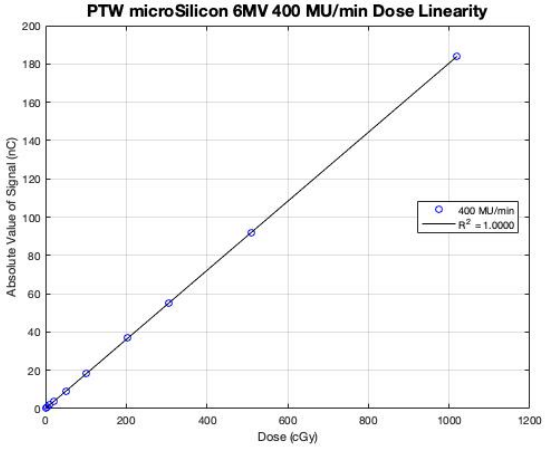

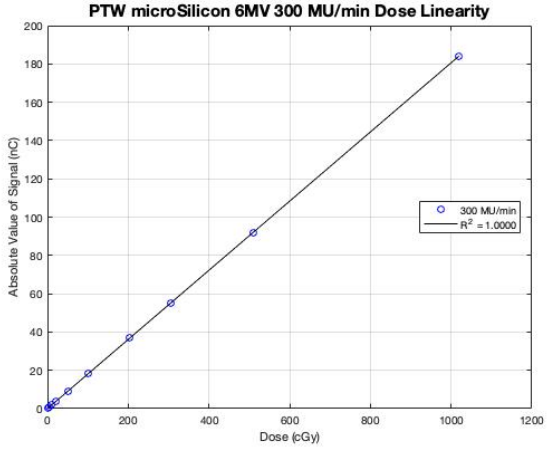

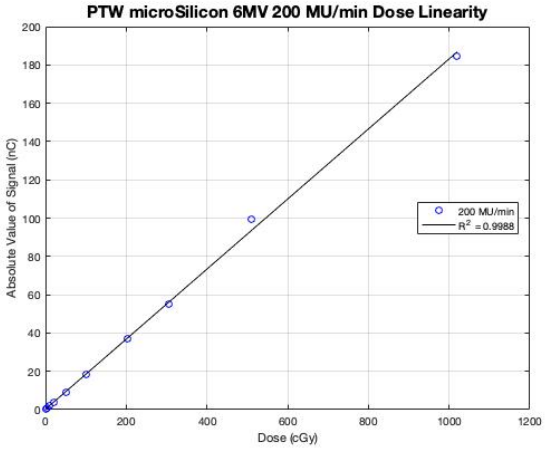

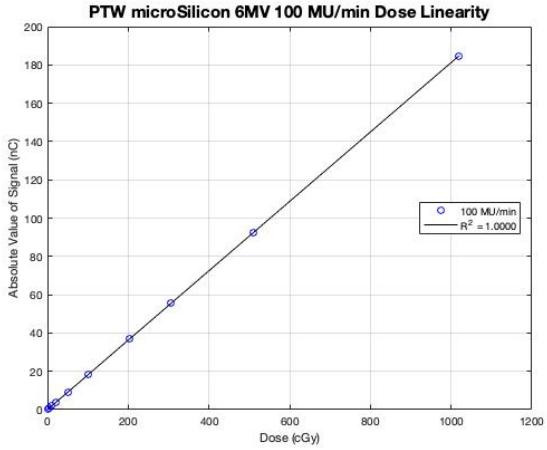

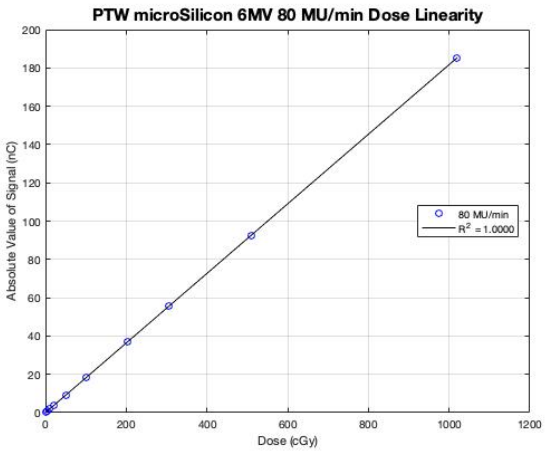
PTW microSilicon 6MV 80 MU/min Dose Linearity
Absolute Value of Signal (nC)
Dose (cGy)
80 MU/min
R² = 1.0000

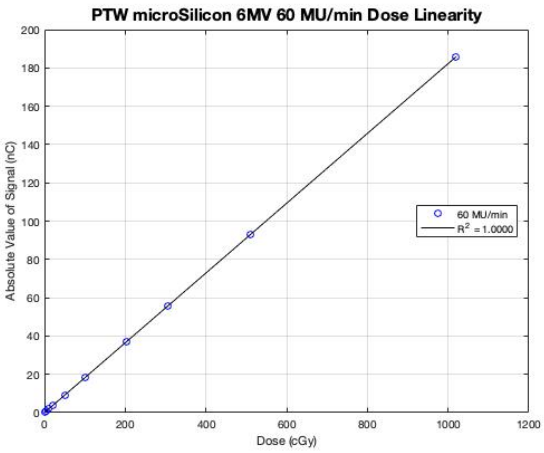
PTW microSilicon 6MV 60 MU/min Dose Linearity
Absolute Value of Signal (nC)
Dose (cGy)
60 MU/min
R² = 1.0000

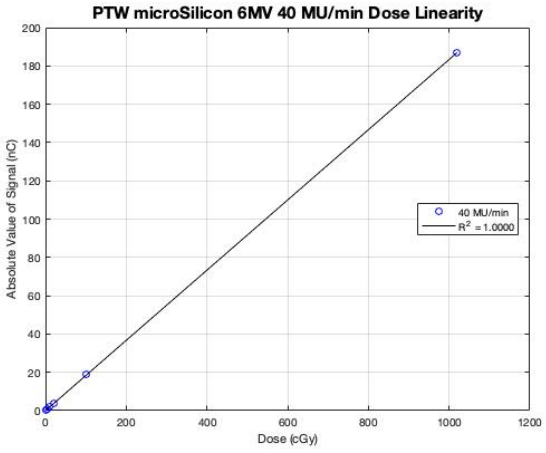
PTW microSilicon 6MV 40 MU/min Dose Linearity
Absolute Value of Signal (nC)
Dose (cGy)
40 MU/min
R² = 1.0000

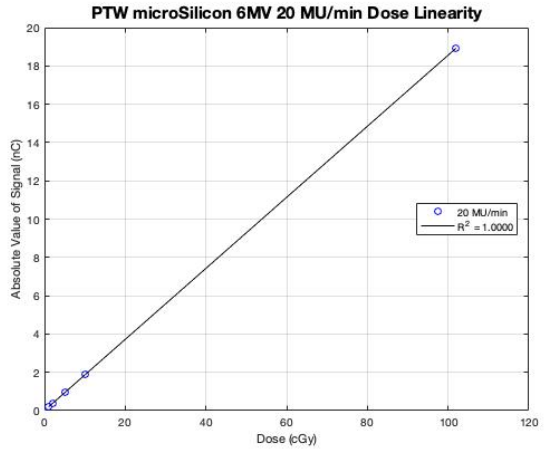
PTW microSilicon 6MV 20 MU/min Dose Linearity
Absolute Value of Signal (nC)
Dose (cGy)
20 MU/min
R² = 1.0000

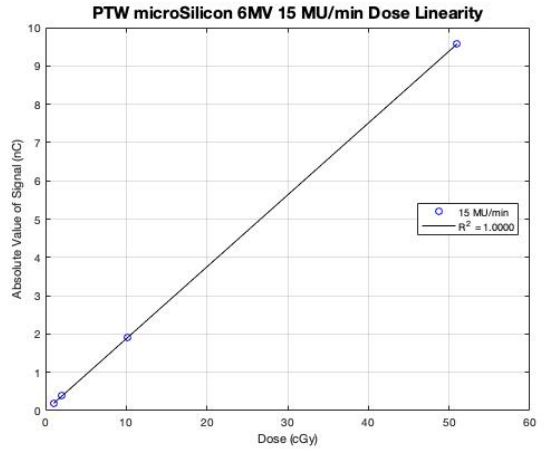
PTW microSilicon 6MV 15 MU/min Dose Linearity
Absolute Value of Signal (nC)
Dose (cGy)
15 MU/min
R² = 1.0000

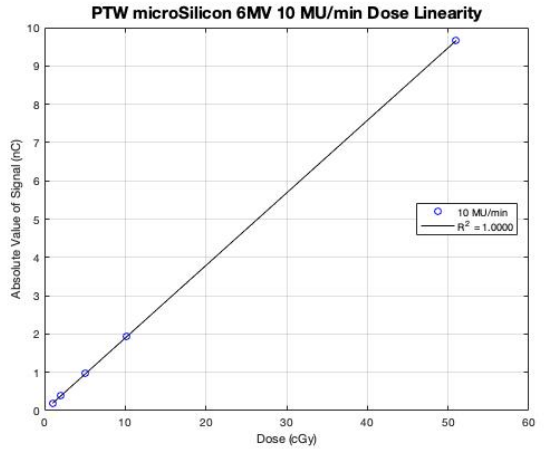
PTW microSilicon 6MV 10 MU/min Dose Linearity
Absolute Value of Signal (nC)
Dose (cGy)
10 MU/min
R² = 1.0000

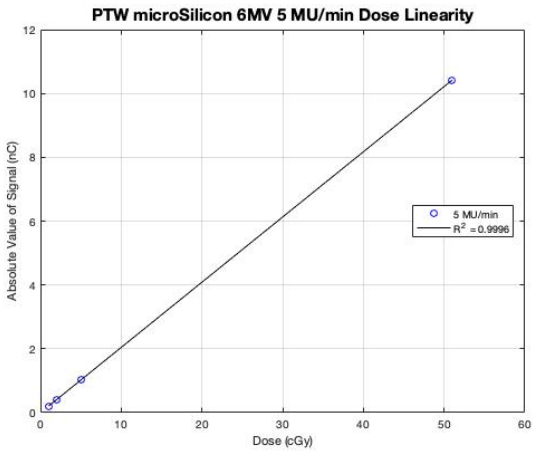

FIG. 19. 6MV dose linearity measurements.

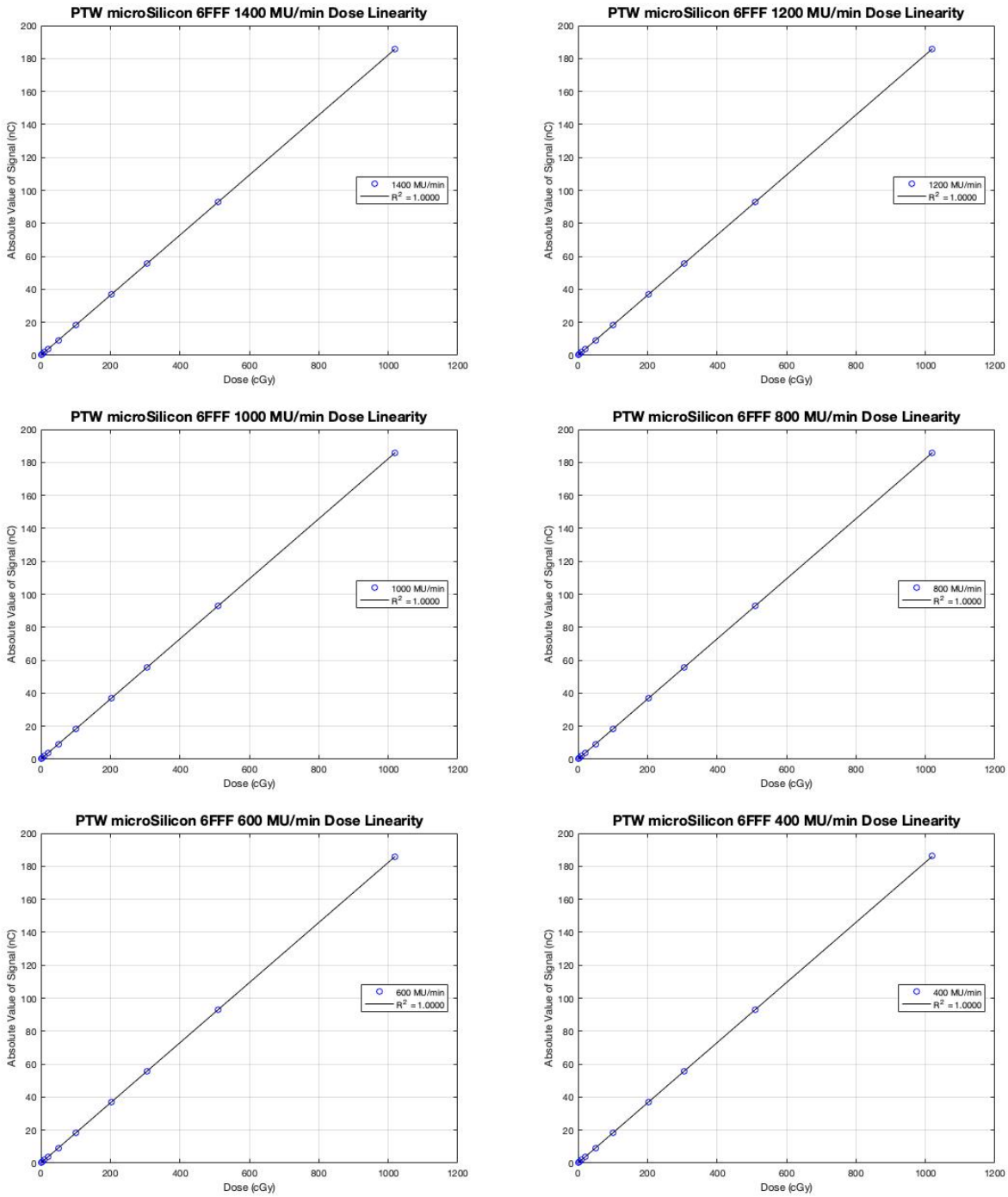

FIG. 20. 6FFF dose linearity measurements.

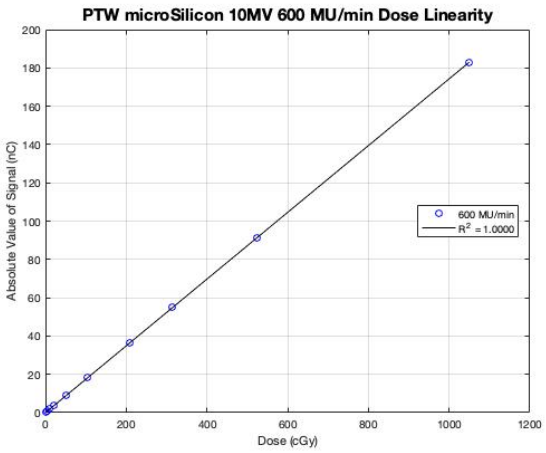
PTW microSilicon 10MV 600 MU/min Dose Linearity
Absolute Value of Signal (nC)
Dose (cGy)
600 MU/min
R² = 1.0000

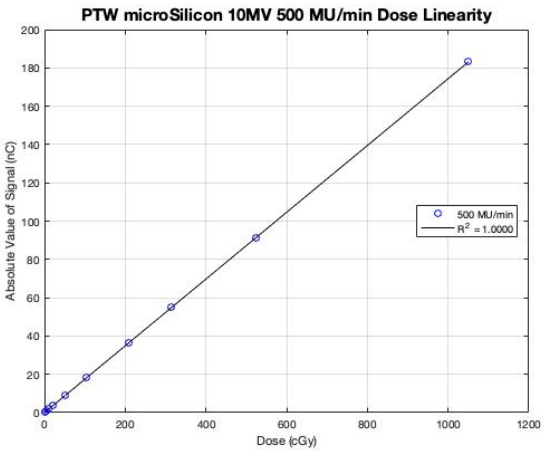
PTW microSilicon 10MV 500 MU/min Dose Linearity
Absolute Value of Signal (nC)
Dose (cGy)
500 MU/min
R² = 1.0000

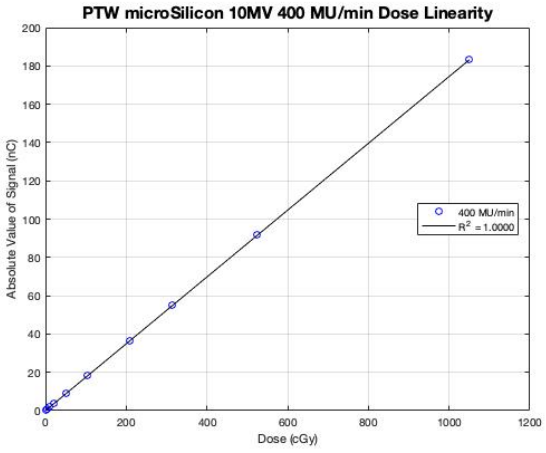
PTW microSilicon 10MV 400 MU/min Dose Linearity
Absolute Value of Signal (nC)
Dose (cGy)
400 MU/min
R² = 1.0000

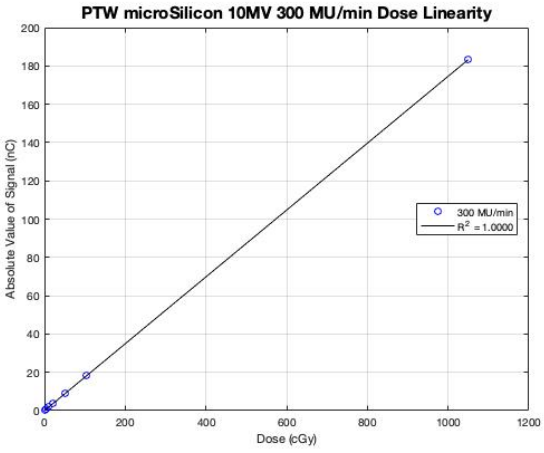
PTW microSilicon 10MV 300 MU/min Dose Linearity
Absolute Value of Signal (nC)
Dose (cGy)
300 MU/min
R² = 1.0000

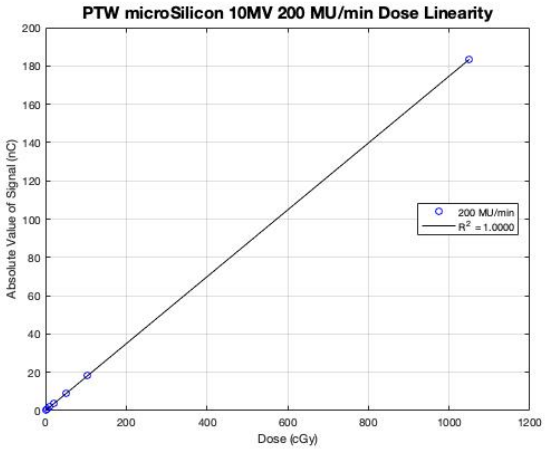
PTW microSilicon 10MV 200 MU/min Dose Linearity
Absolute Value of Signal (nC)
Dose (cGy)
200 MU/min
R² = 1.0000

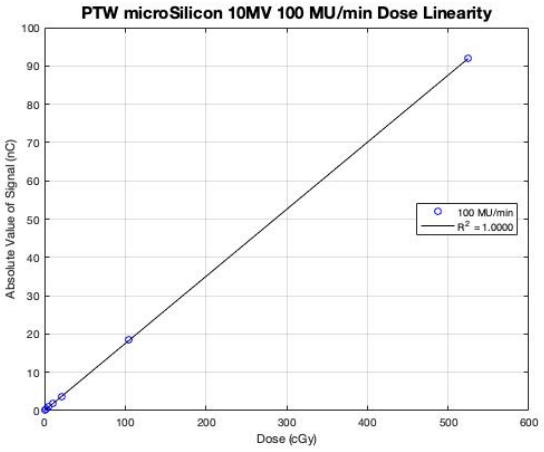
PTW microSilicon 10MV 100 MU/min Dose Linearity
Absolute Value of Signal (nC)
Dose (cGy)
100 MU/min
R² = 1.0000

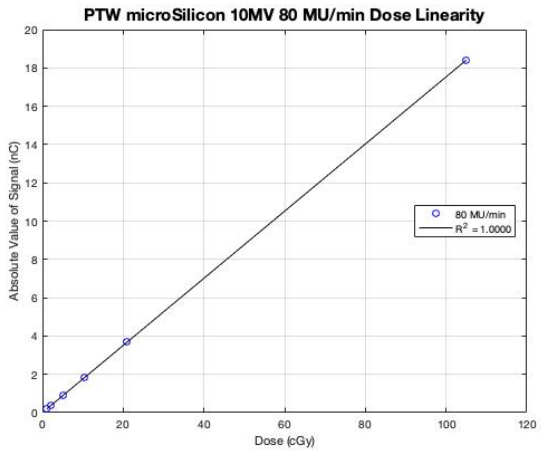
PTW microSilicon 10MV 80 MU/min Dose Linearity
Absolute Value of Signal (nC)
Dose (cGy)
80 MU/min
R² = 1.0000

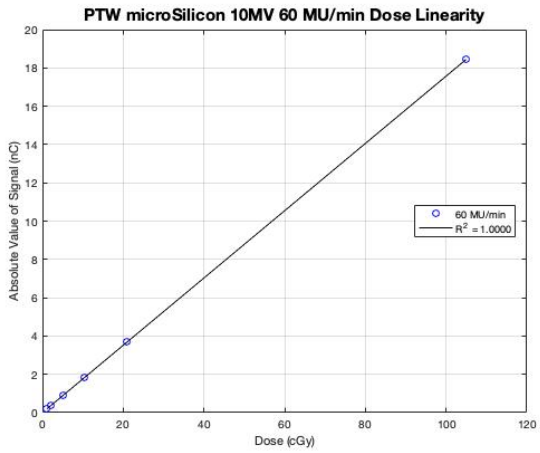
PTW microSilicon 10MV 60 MU/min Dose Linearity
Absolute Value of Signal (nC)
Dose (cGy)
60 MU/min
R² = 1.0000

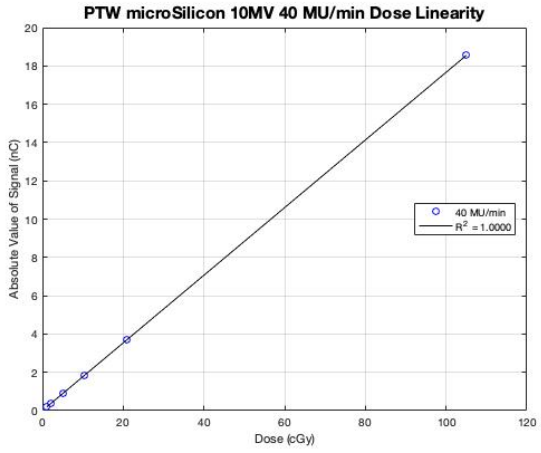
PTW microSilicon 10MV 40 MU/min Dose Linearity
Absolute Value of Signal (nC)
Dose (cGy)
40 MU/min
R² = 1.0000

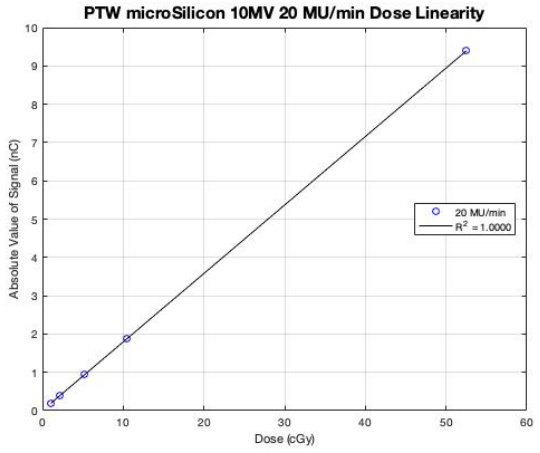
PTW microSilicon 10MV 20 MU/min Dose Linearity
Absolute Value of Signal (nC)
Dose (cGy)
20 MU/min
R² = 1.0000

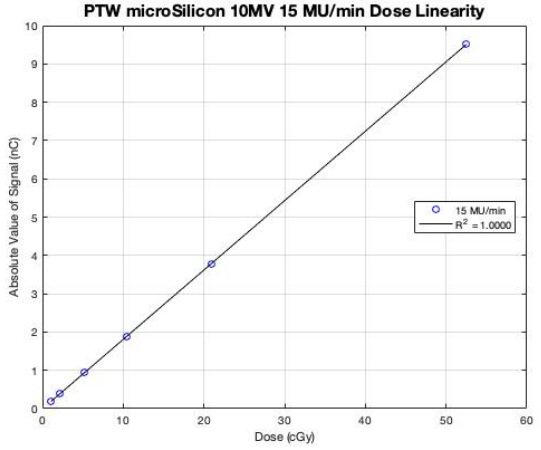
PTW microSilicon 10MV 15 MU/min Dose Linearity
Absolute Value of Signal (nC)
Dose (cGy)
15 MU/min
R² = 1.0000

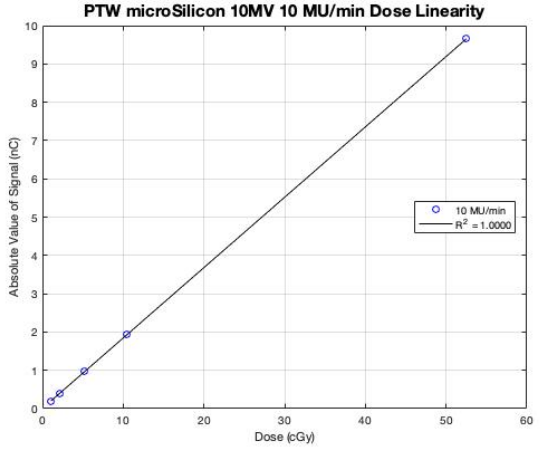
PTW microSilicon 10MV 10 MU/min Dose Linearity
Absolute Value of Signal (nC)
Dose (cGy)
10 MU/min
R² = 1.0000

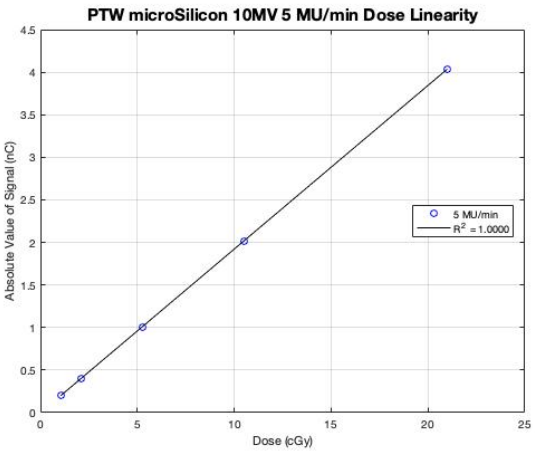

FIG. 21. 10MV dose linearity measurements.

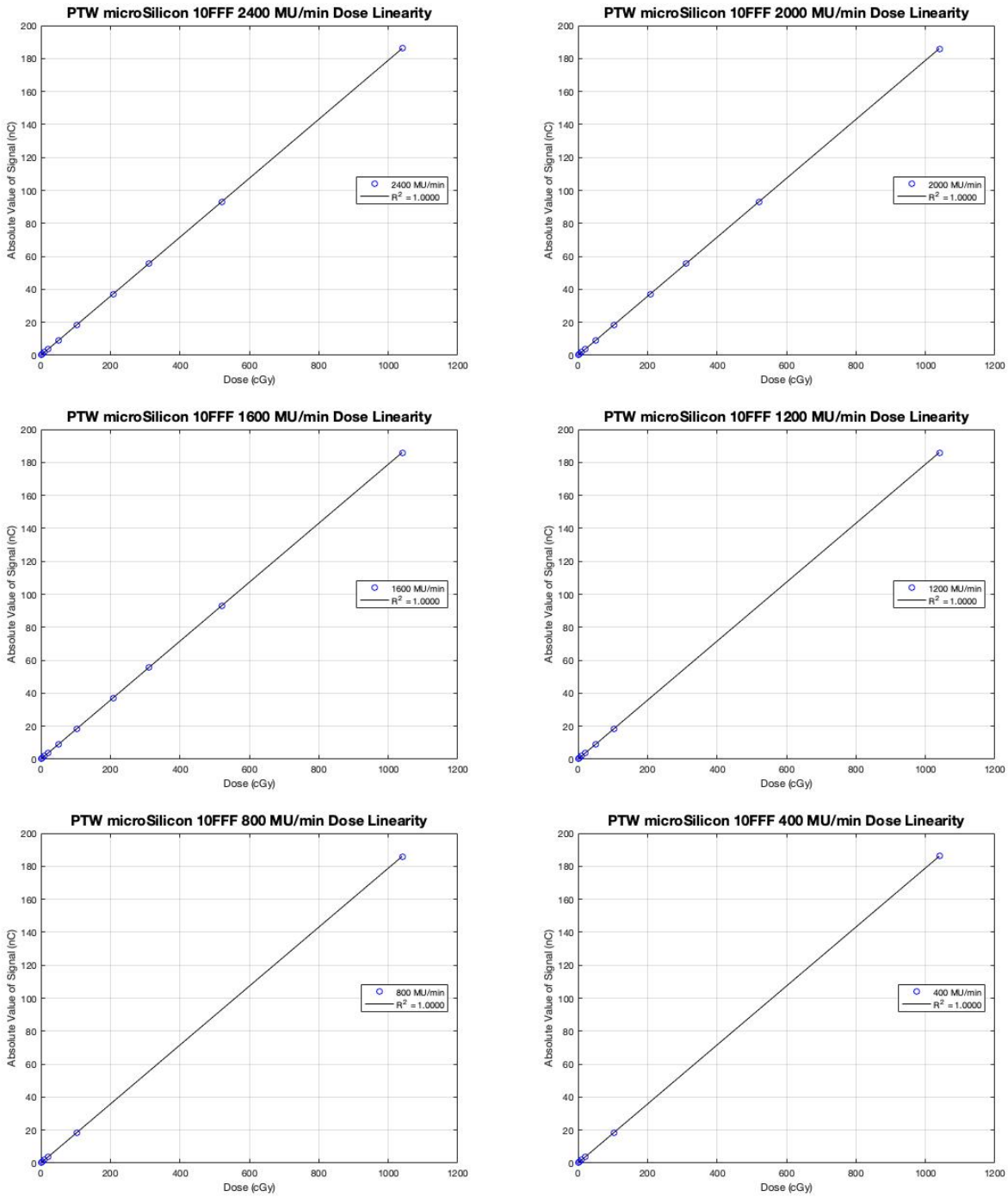

FIG. 22. 10FFF dose linearity measurements.

10.2 Small field profiles

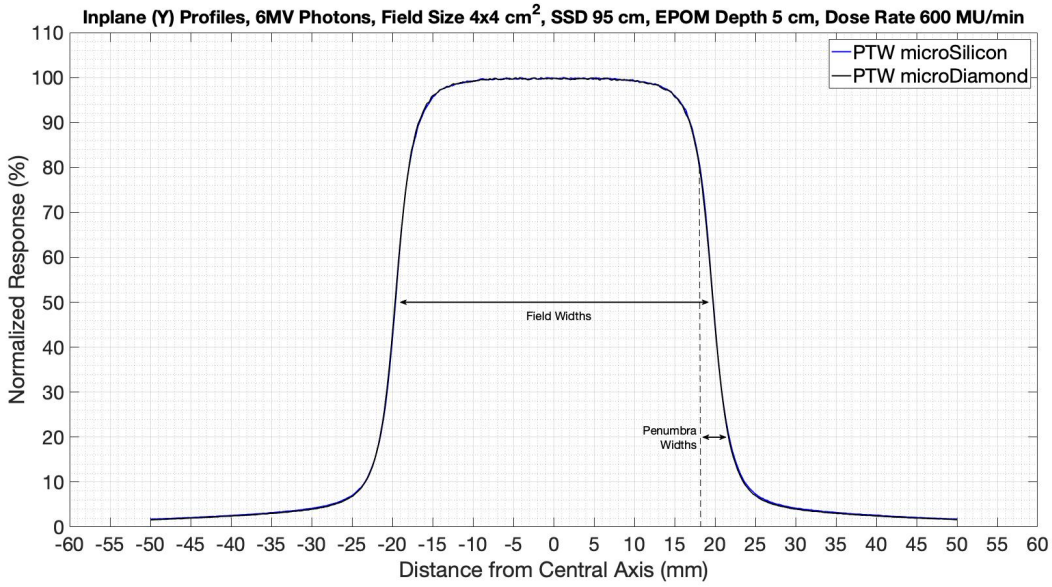

FIG. 23. 6MV 4 x 4 cm^2 field size inplane profile measurements.

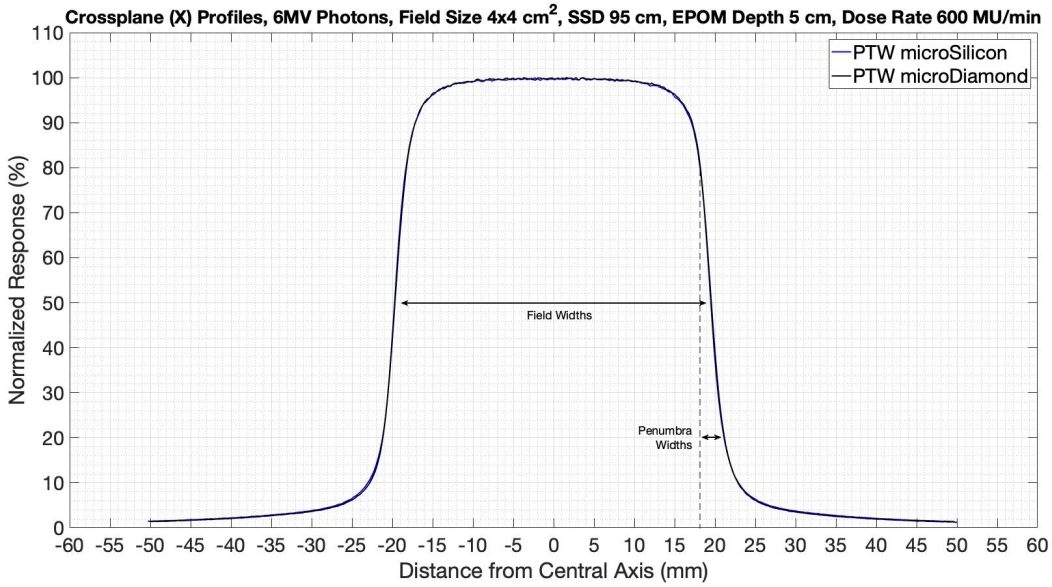

FIG. 24. 6MV 4 x 4 cm^2 field size crossplane profile measurements.

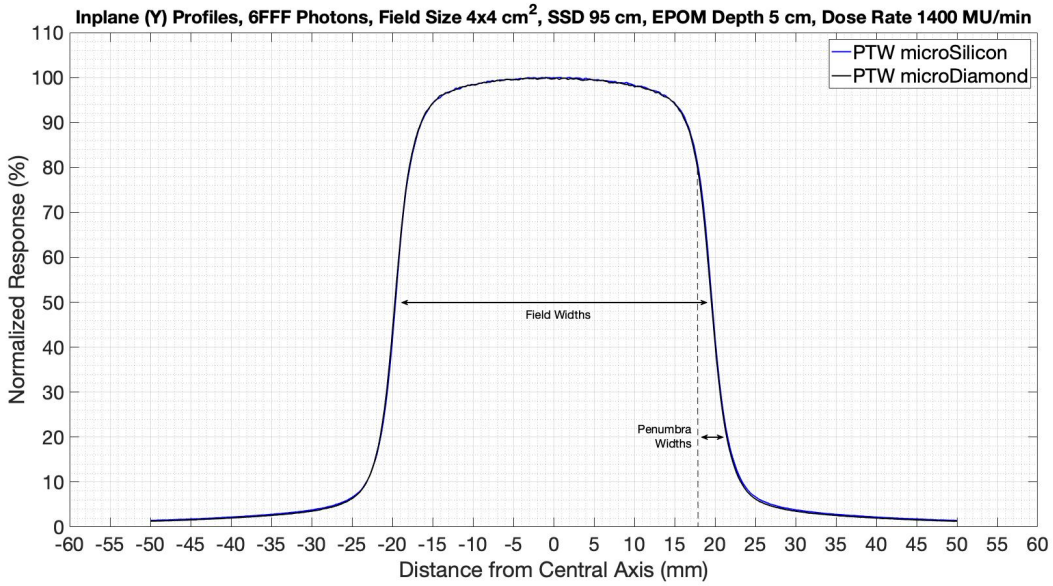

FIG. 25. 6FFF 4 x 4 cm^2 field size inplane profile measurements.

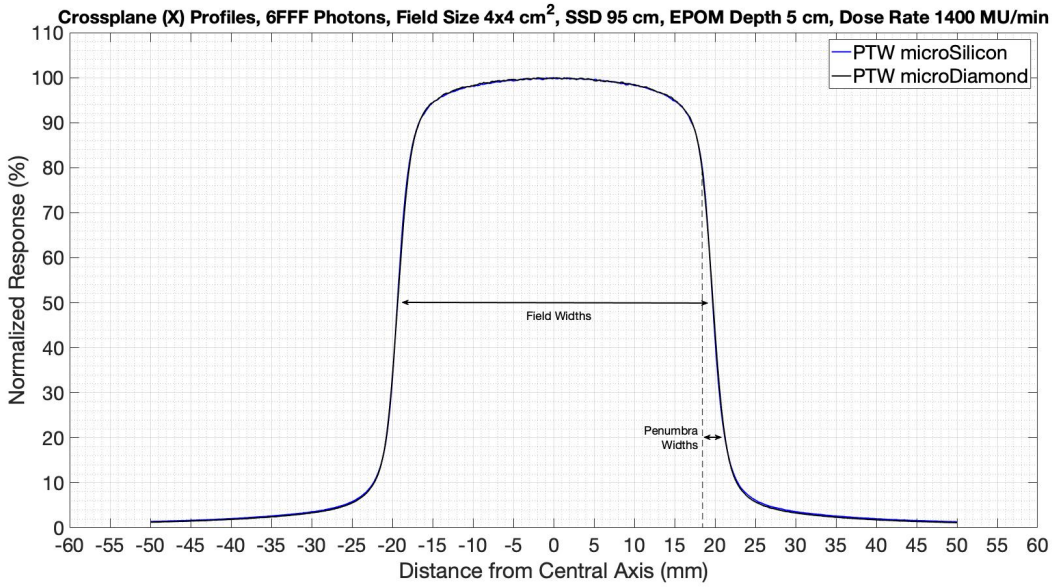

FIG. 26. 6FFF 4 x 4 cm^2 field size crossplane profile measurements.

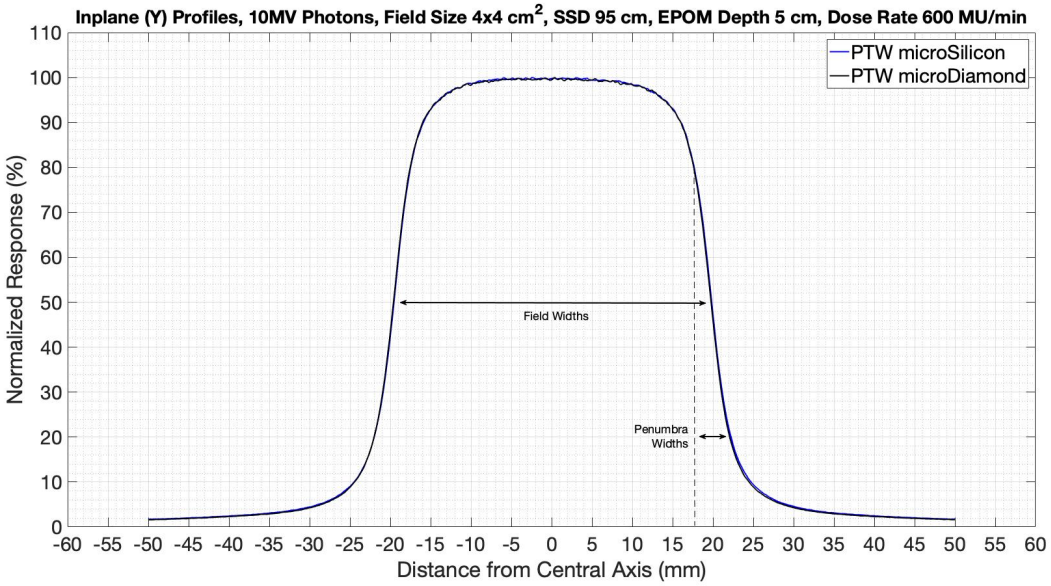

FIG. 27. 10MV 4 x 4 cm^2 field size inplane profile measurements.

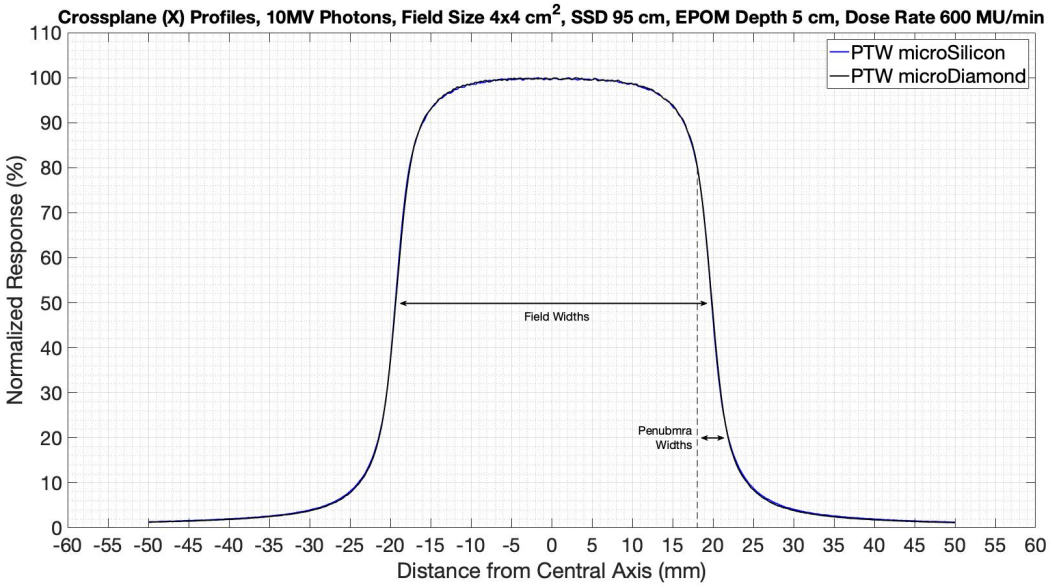

FIG. 28. 10MV 4 x 4 cm^2 field size crossplane profile measurements.

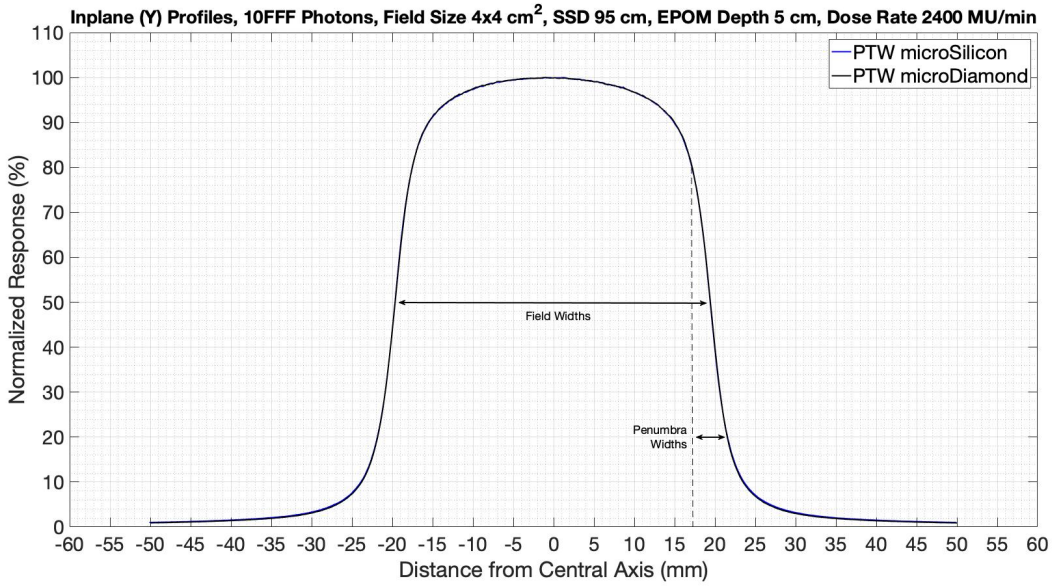

FIG. 29. 10FFF 4 x 4 cm^2 field size inplane profile measurements.

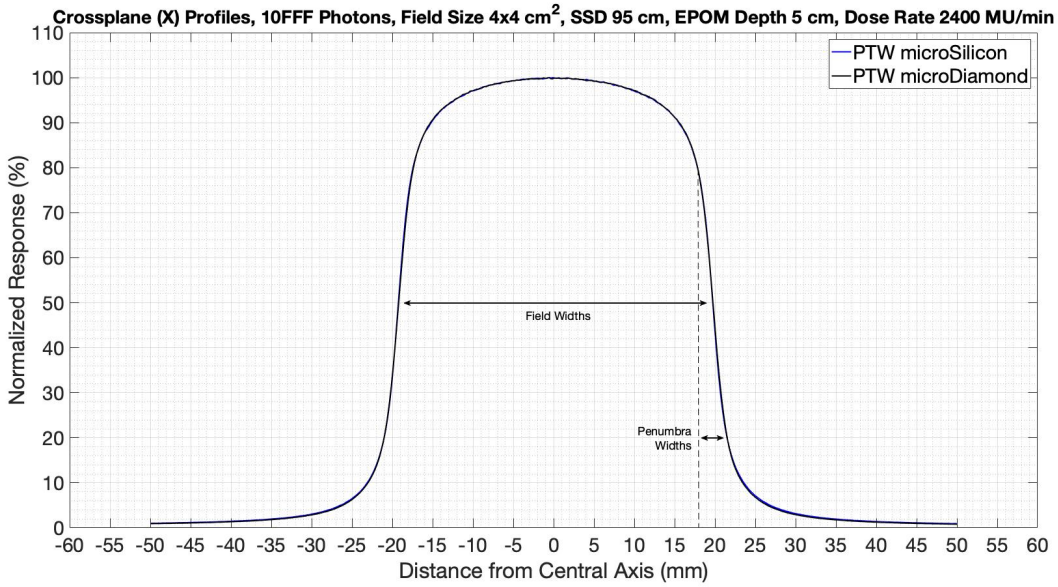

FIG. 30. 10FFF 4 x 4 cm^2 field size crossplane profile measurements.

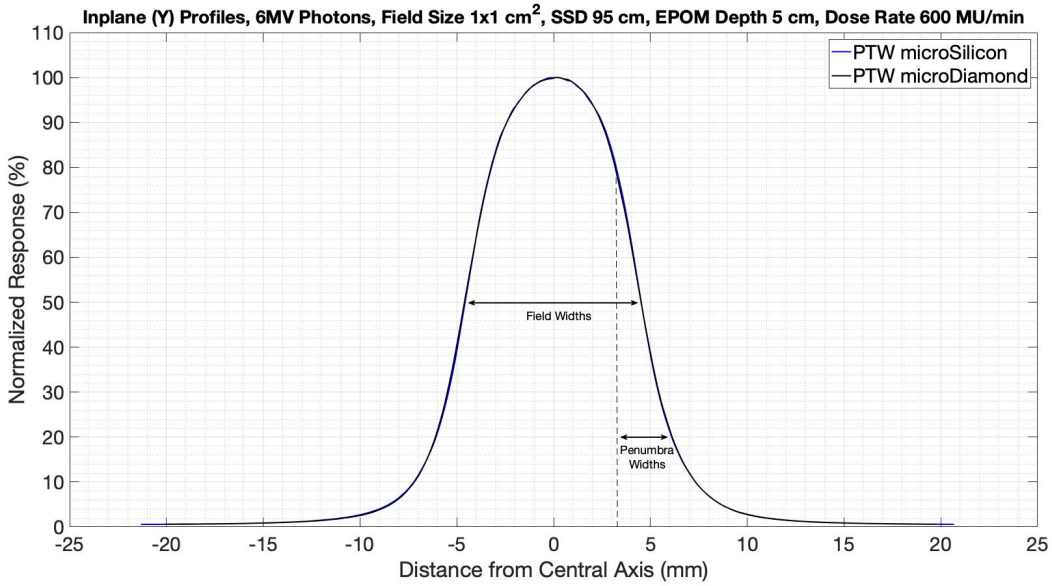

FIG. 31. 6MV 1 x 1 cm^2 field size inplane profile measurements.

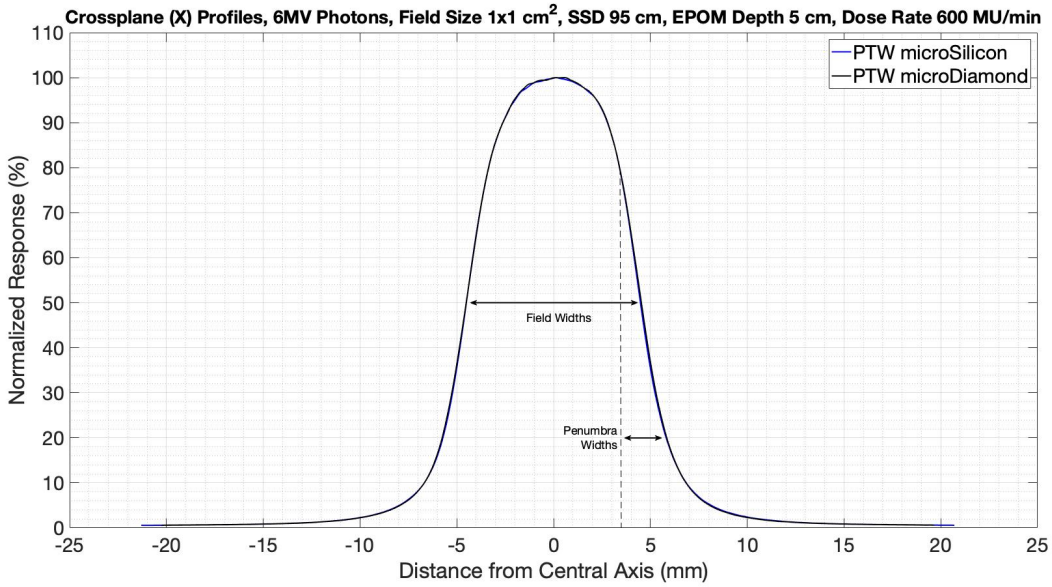

FIG. 32. 6MV 1 x 1 cm^2 field size crossplane profile measurements.

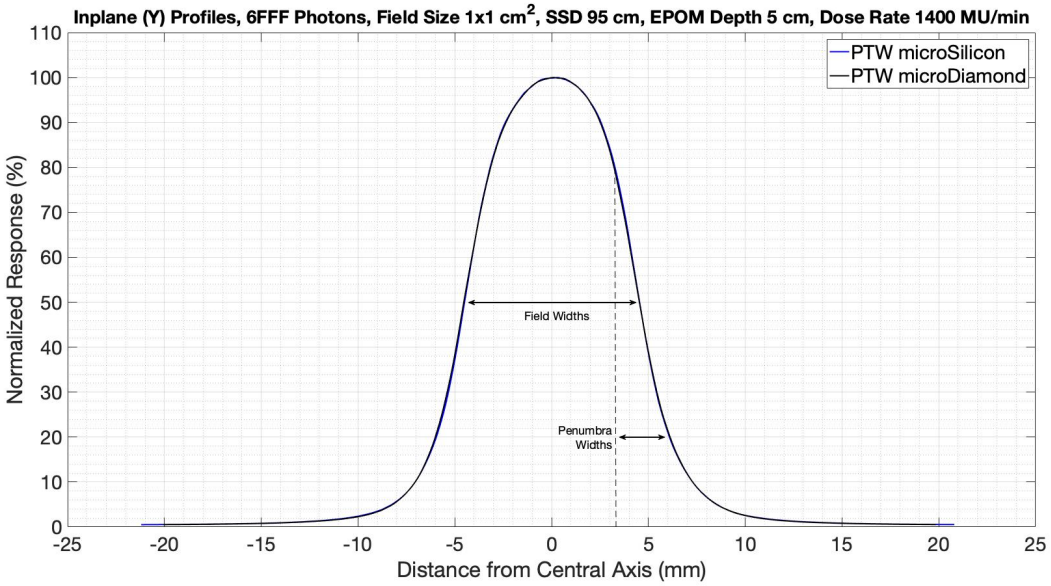

FIG. 33. 6FFF 1 x 1 cm^2 field size inplane profile measurements.

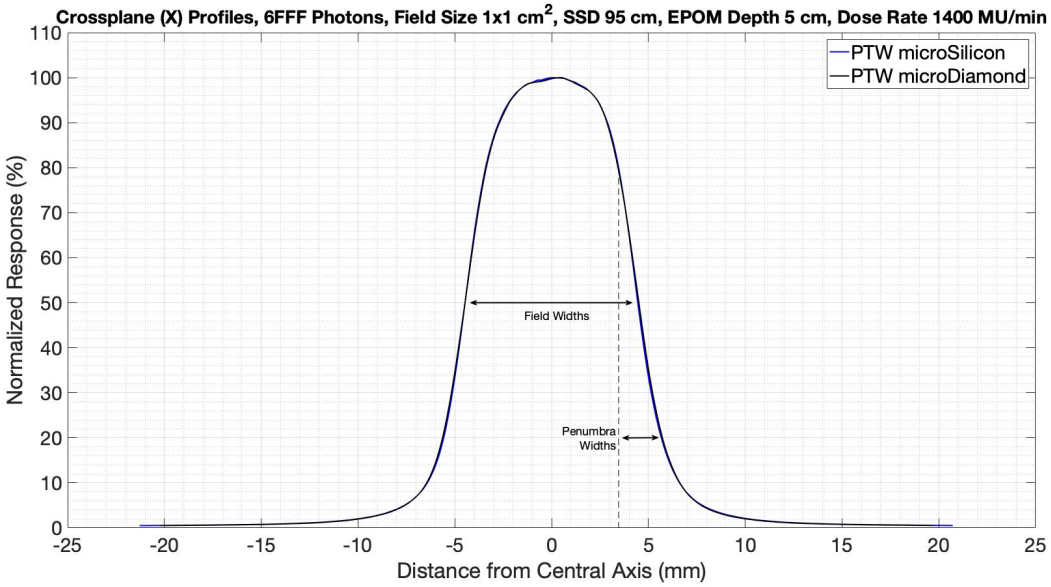

FIG. 34. 6FFF 1 x 1 cm^2 field size crossplane profile measurements.

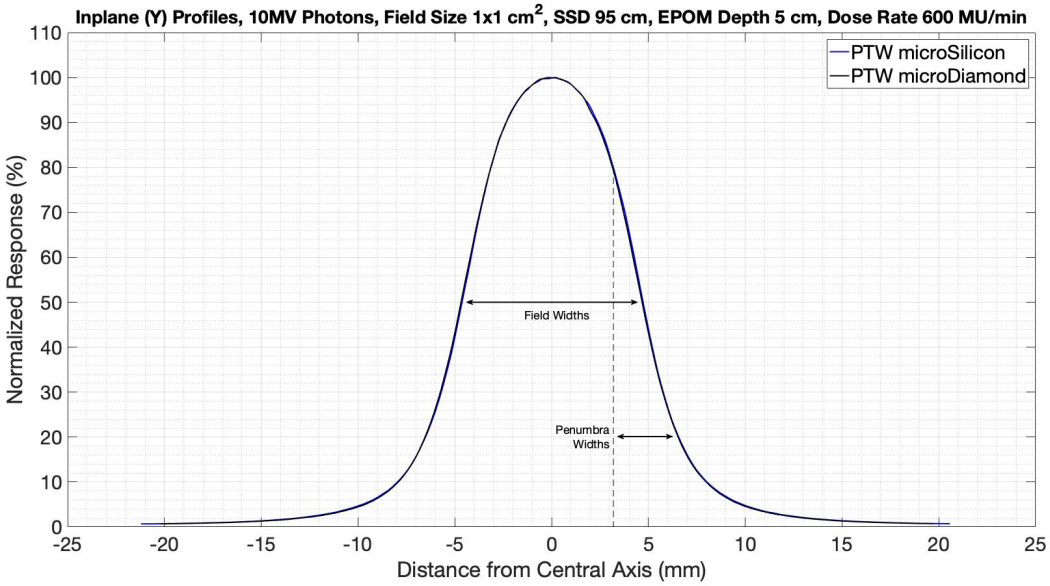

FIG. 35. 10MV 1 x 1 cm^2 field size inplane profile measurements.

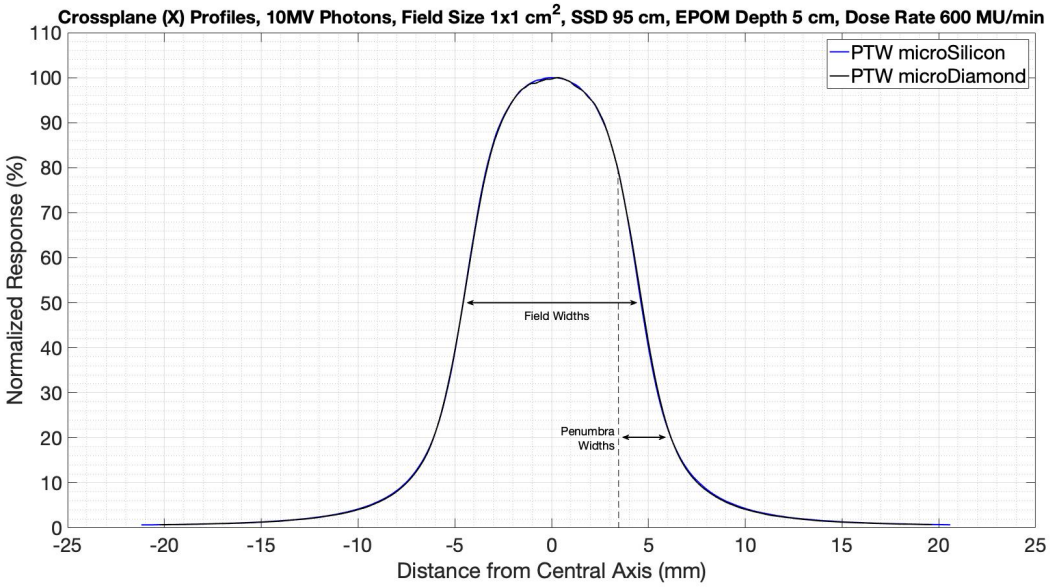

FIG. 36. 10MV 1 x 1 cm^2 field size crossplane profile measurements.

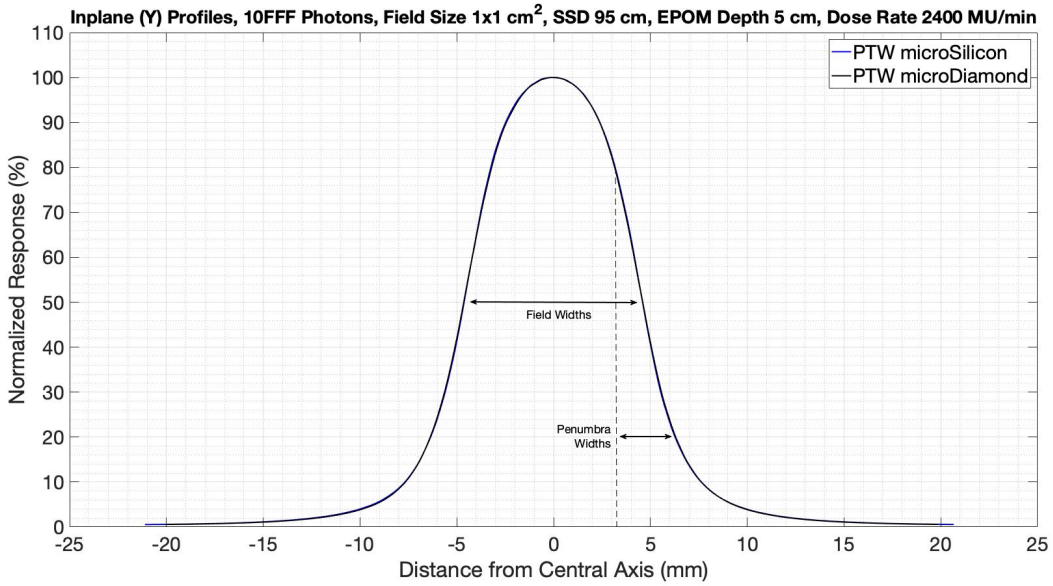

FIG. 37. 10FFF 1 x 1 cm^2 field size inplane profile measurements.

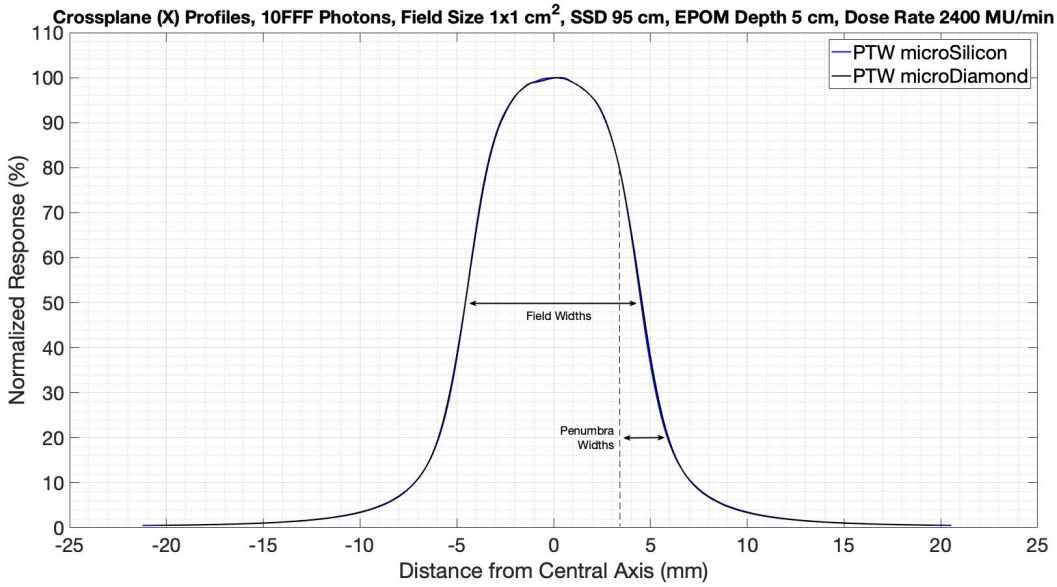

FIG. 38. 10FFF 1 x 1 cm^2 field size crossplane profile measurements.

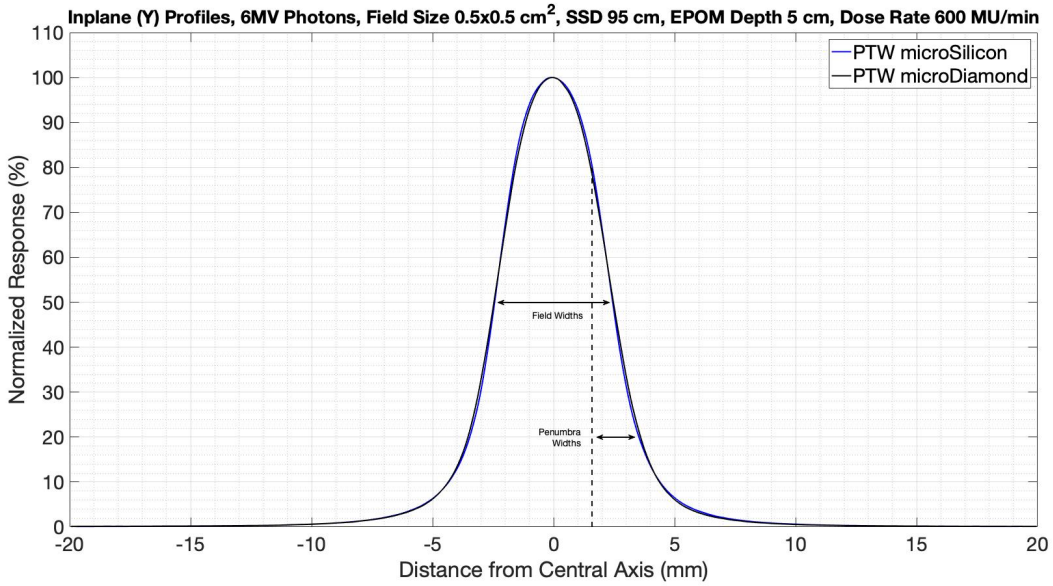

FIG. 39. 6MV 0.5 x 0.5 cm^2 field size inplane profile measurements.

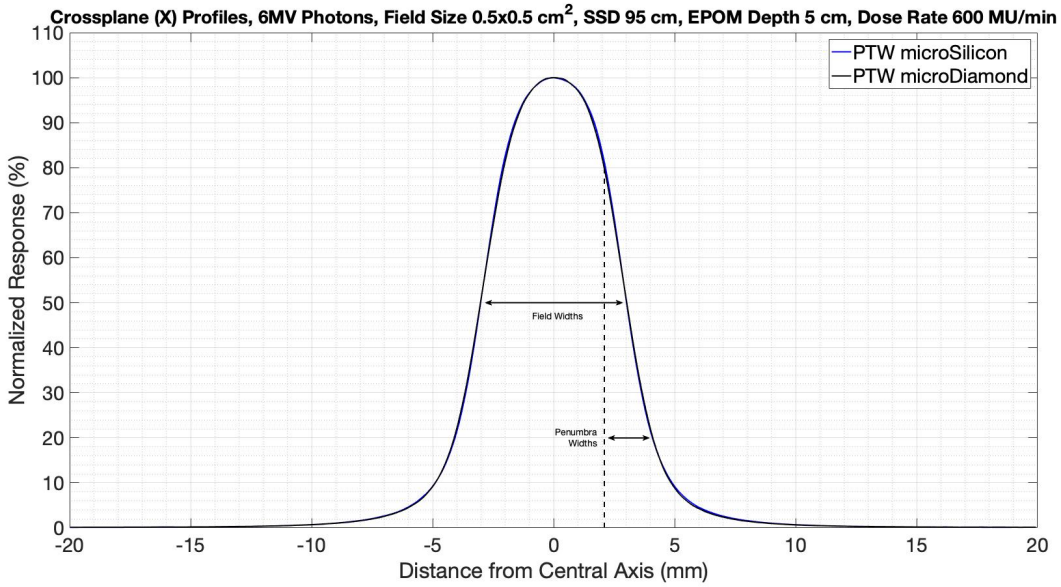

FIG. 40. 6MV 0.5 x 0.5 cm^2 field size crossplane profile measurements.

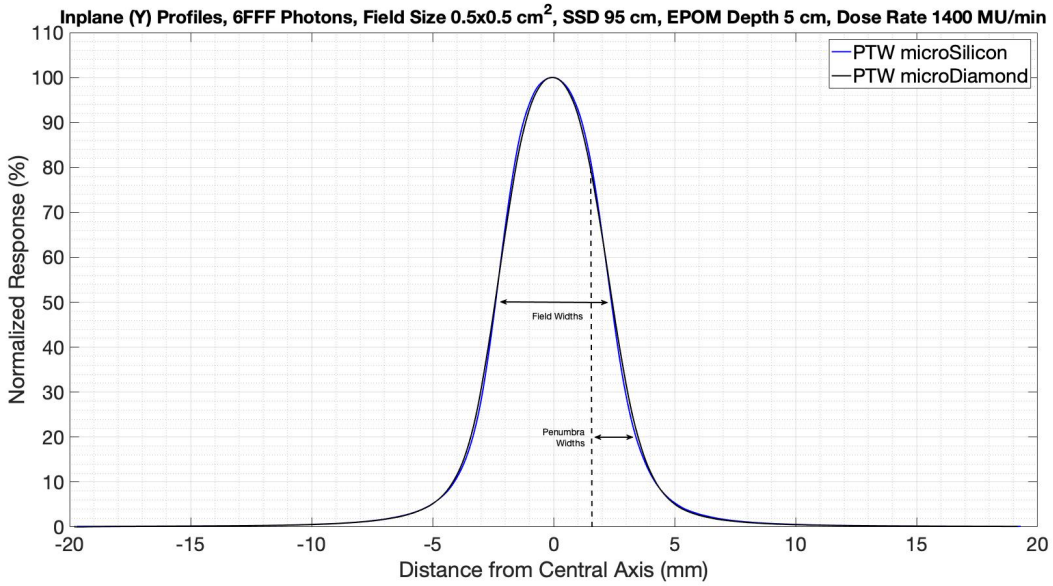

FIG. 41. 6FFF 0.5 x 0.5 cm^2 field size inplane profile measurements.

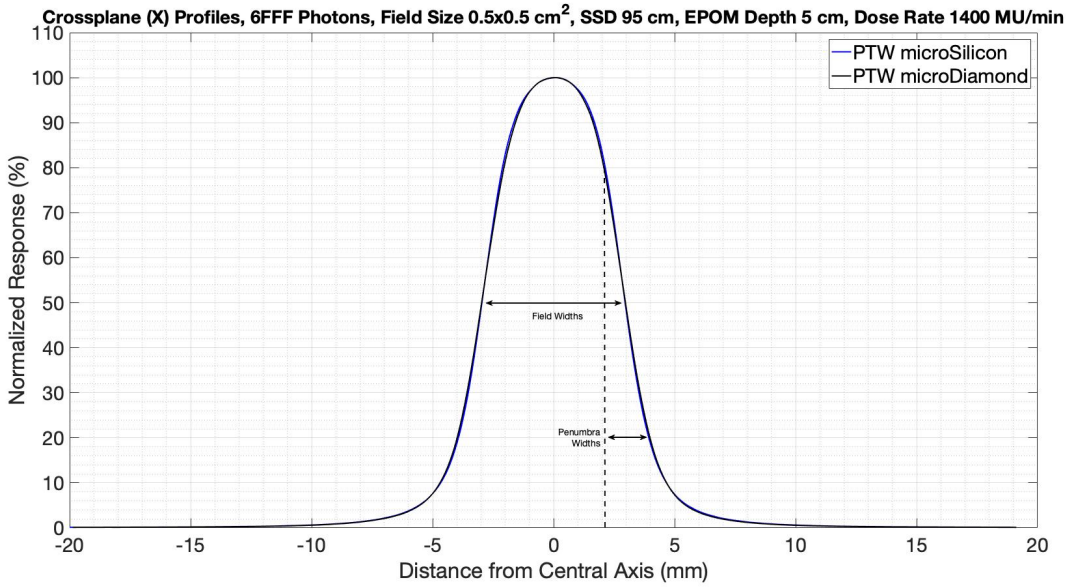

FIG. 42. 6FFF 0.5 x 0.5 cm^2 field size crossplane profile measurements.

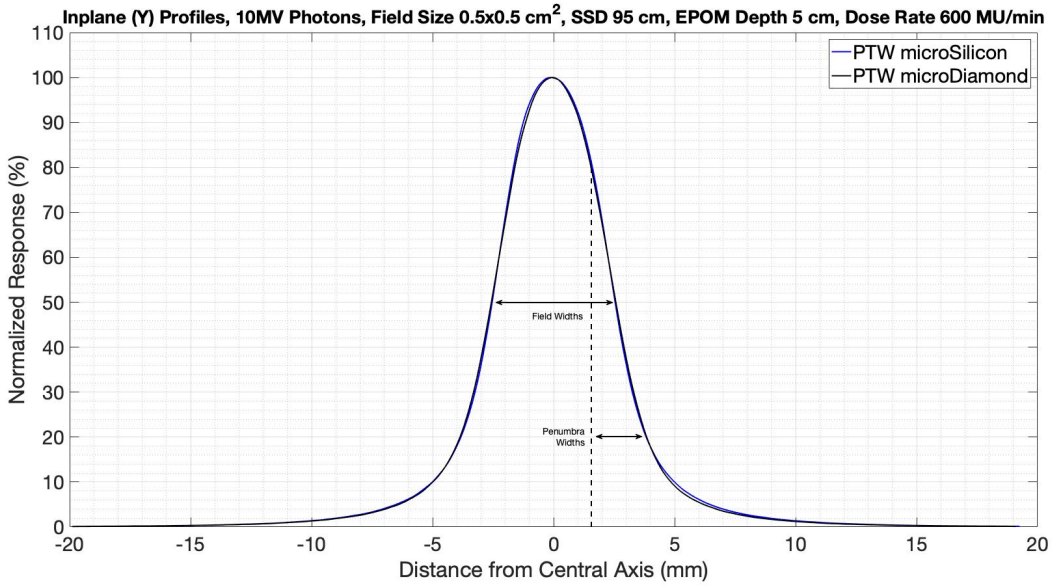

FIG. 43. 10MV 0.5 x 0.5 cm^2 field size inplane profile measurements.

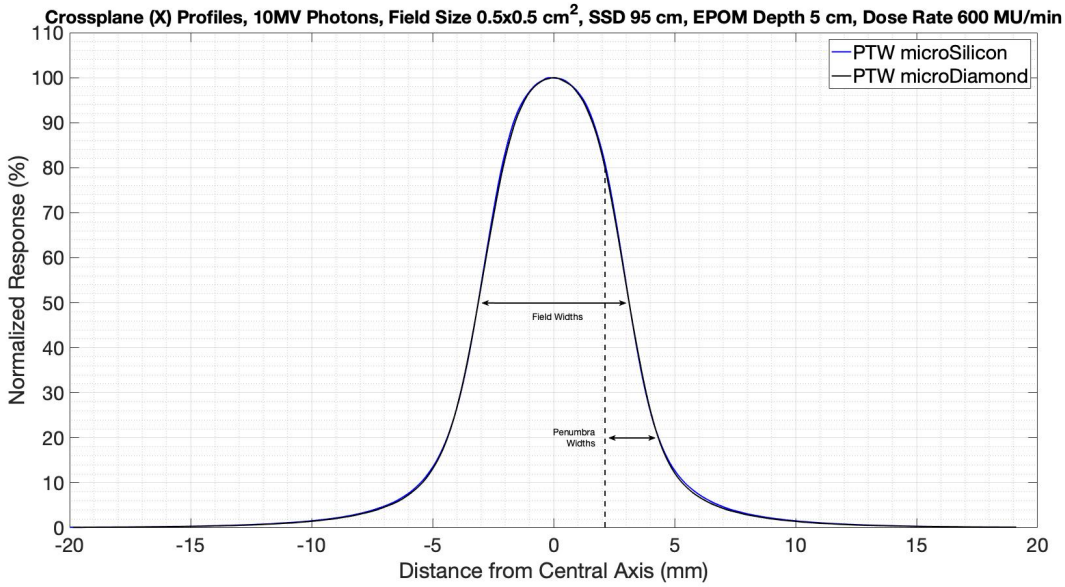

FIG. 44. 10MV 0.5 x 0.5 cm^2 field size crossplane profile measurements.

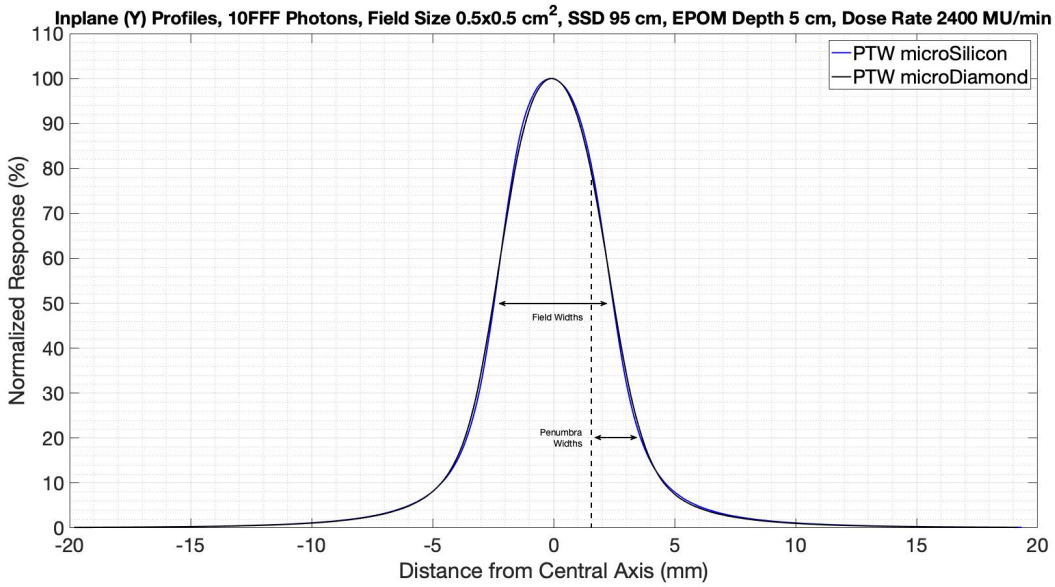

FIG. 45. 10FFF 0.5 x 0.5 cm^2 field size inplane profile measurements.

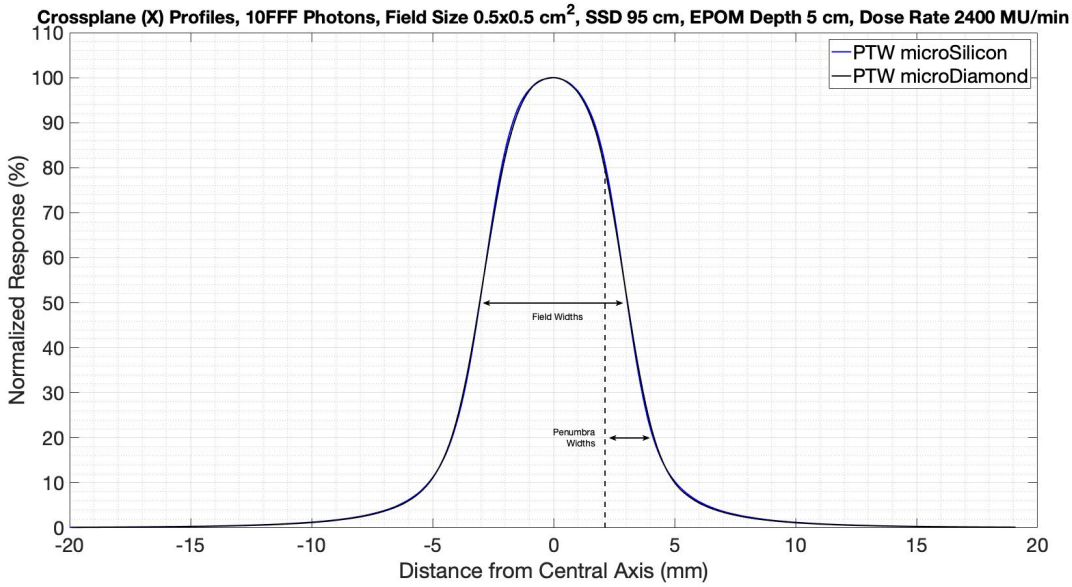

FIG. 46. 10FFF 0.5 x 0.5 cm^2 field size crossplane profile measurements.